November 14, 2023

Collective incentives reduce over-exploitation of social information in unconstrained human groups

Dominik Deffner[1,2*], David Mezey[2,3], Benjamin Kahl[1], Alexander Schakowski[1], Pawel Romanczuk[2,3], Charley M. Wu[1,4,5] & Ralf H.J.M. Kurvers[1,2]

[1]Center for Adaptive Rationality, Max Planck Institute for Human Development, Berlin, Germany
[2]Science of Intelligence Excellence Cluster, Technical University Berlin, Berlin, Germany
[3]Institute for Theoretical Biology, Humboldt University Berlin, Berlin, Germany
[4]University of Tübingen, Tübingen, Germany
[5]Max Planck Institute for Biological Cybernetics, Tübingen, Germany
*deffner@mpib-berlin.mpg.de

ABSTRACT

Collective dynamics emerge from countless individual decisions. Yet, we poorly understand the processes governing dynamically-interacting individuals in human collectives under realistic conditions. We present a naturalistic immersive-reality experiment where groups of participants searched for rewards in different environments, studying how individuals weigh personal and social information and how this shapes individual and collective outcomes. Capturing high-resolution visual-spatial data, behavioral analyses revealed individual-level gains—but group-level losses—of high social information use and spatial proximity in environments with concentrated (vs. distributed) resources. Incentivizing participants at the group (vs. individual) level facilitated adaptation to concentrated environments, buffering apparently excessive scrounging. To infer discrete choices from unconstrained interactions and uncover the underlying decision mechanisms, we developed an unsupervised Social Hidden Markov Decision model. Computational results showed that participants were more sensitive to social information in concentrated environments frequently switching to a 'social relocation' state where they approach successful group members. Group-level incentives reduced participants' overall responsiveness to social information and promoted higher selectivity over time. Finally, mapping group-level spatio-temporal dynamics through time-lagged regressions revealed a collective exploration-exploitation trade-off across different timescales. Our study unravels the processes linking individual-level strategies to emerging collective dynamics, and provides new tools to investigate decision-making in freely-interacting collectives.

Key words. Social information use, decision-making, collective dynamics, Hidden Markov models, social learning

1. Introduction

Collective behavior emerges from individual-level cognition, and the cognitive mechanisms driving social interactions strongly determine whether social influence promotes adaptive behavior or leads to maladaptive herding [1, 2]. Despite their crucial role in governing the outcomes of collective behaviors, the decision-making processes of human collectives under naturalistic conditions remain poorly understood [3, 4].

One of the key trade-offs driving collective systems is between using personal versus social information. Relying too heavily on personal information prevents the spread of useful information, while relying too heavily on social information reduces exploration and generates over-exploitation of the environment [5–9]. This trade-off is key across social contexts, from social foraging [10], to the discovery of new tools [11, 12], or computer code [13], to the planting of crops [14, 15]. In all such situations, individuals must continuously integrate their personal information with information acquired from others and make strategic decisions on different timescales. The mechanistic underpinnings of these processes are, however, still largely unknown.

Most experimental studies to date on social decision-making used static—and often simulated—sources of social information [7] or let interacting participants choose among a small set of well-defined options at prespecified time points [e.g., 14–18]. To understand the mechanisms governing real-world human collective systems, we need paradigms that allow complex social dynamics to unfold within naturalistic environments. Analyzing behavior in such complex systems requires novel computational models that describe how dynamically-interacting individuals make decisions while accounting for their unique (visual) perspectives and spatial constraints [2, 19, 20]. Such constraints are unavoidable features of the real world and

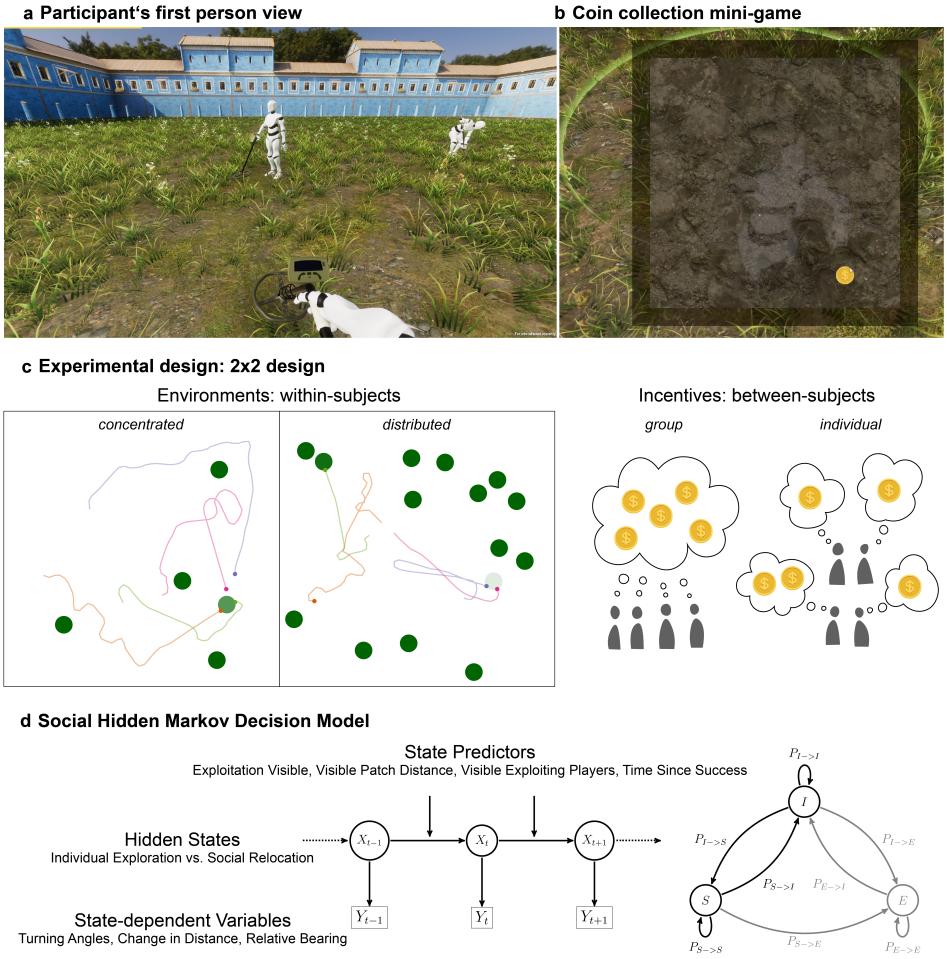

Fig. 1: **Collective foraging task and Social Hidden Markov Decision model**. (a) Participants in groups of four searched for circular research patches in a square environment. A metal detector lighted up when they have discovered a patch. Participants could observe each other in real time and decide to join other players who have discovered a patch (exploiting players indicated by digging animation; see avatar on the right). (b) Once participants have discovered a patch or joined others, they started extracting coins in a mini-game by clicking on coin symbols appearing on the screen in a 2-second interval. (c) Participants completed four rounds of the task in a 2x2 experimental design. Each group conducted two rounds in a *concentrated* environment (5 patches with 48 coins each) and two rounds in a *distributed* environment (15 patches with 16 coins each). Colored dots and lines represent snapshots of the current position of four players as well as their movement trajectories in the last minute. Lighter green patches have fewer coins left. Half of the groups were incentivized on the *group* level and half of the groups were incentivized on the *individual* level. (d) Our computational approach uses state-dependent variables to assign participants to hidden states at each time point: "Individual Exploration" (I; independently search for resource patches) or "Social Relocation" (S; use social information and approach successful group members). The model simultaneously infers the transition probabilities between latent states (as "Exploitation" E is known, we only need to explicitly model transitions between I and S). We model the (time-dependent) influence of state predictors on the probability to stop exploring and switch to social relocation, $P_{I->S}$ (see Eq. 1).

fundamentally shape the costs and benefits of social information use [19, 21]; they are thus prerequisites for testing collective dynamics in more realistic settings and connecting abstract models to reality.

Here, we use an immersive-reality approach to study how groups of four participants search for resources ("coins") in a 3D virtual environment with different resource distributions and incentive structures. Participants could observe each other in real time and decide to join players who successfully discovered a resource patch (Fig. 1a; Supplementary Video 1). The 3D environment imposes a limited, first-person, field of view as well as realistic spatial constraints creating a natural trade-off between individual exploration of the environment and social information use [20, 22]. Participants completed four rounds of the task in a 2x2 design (Fig. 1c; see Methods). In half of the rounds, resource units were *concentrated* in relatively few—but rich—

patches. In the other rounds, the same number of units were *distributed* among many—but poorer—patches. Theory on producer-scrounger games [e.g., 5, 10, 23–26] predicts that a "scrounging" strategy, where agents use social information to join resource patches discovered by others, increases in frequency (relative to individually-searching "producers") when patches are difficult to find but rich in resources. Therefore, we expected participants to rely more on social information and to be less selective in concentrated compared to distributed environments.

Across social systems, individual incentives do not always align with the interest of the collective and theory on producer-scrounger dynamics [5, 10, 24–26], and the evolution of social learning [6, 27] predicts that social information use can be individually beneficial while at the same time reducing collective performance or population fitness. To investigate how participants balance the pros and cons of social information use depending on their interdependence with others, half of the groups were incentivized on the group level (i.e., paid depending on group success), while the other half on the individual level (i.e., paid depending on personal success). Since scroungers capitalize on others' discoveries and compete for limited local resources, we expected participants to rely less on social information when incentivized on the group level reducing maladaptive over-exploitation of social information (see preregistration for the full set of predictions: https://osf.io/5r736/).

Our analyses leveraged high-resolution time-series data from each participant of their visual information and movement trajectories. Behavioral analyses revealed individual-level benefits of high social information use and spatial proximity in concentrated resource environments, which came at the expense of group performance. Crucially, group-level incentives alleviated the negative consequences of apparently excessive scrounging. We next developed an unsupervised *Social Hidden Markov Decision model* (inspired by animal movement models in ecology [28, 29]) to simultaneously infer decision sequences between latent states and describe how resource distributions, incentives, and situational factors influence participants' decisions to use social information (Fig. 1d). Quantifying such latent social decision-making, we uncovered the mechanisms underlying behavioral outcomes, demonstrating how participants strategically adjusted their social information use to both environmental demands and incentive structure. Group incentives facilitated adaptive tuning of decision strategies over time, with increased selectivity acting as a safeguard against maladaptive over-reliance on social information. Finally, we mapped the emerging group-level spatio-temporal dynamics through time-lagged Gaussian process regressions and discovered consistent collective benefits of more individualistic search in distributed environments and a collective exploration-exploitation trade-off in concentrated environments.

2. Results

We start by examining participants' behavior before turning to computational analyses. Results are reported as population-level effects from hierarchical Bayesian models controlling for participant- and group-level variability in both intercepts and slopes (for frequentist analyses of main behavioral results producing identical conclusions, see Supplementary Tables 1-7). Inferences are based on posterior contrasts between conditions (on the outcome scale for behavior, on a latent scale for computational results), reported as posterior means and 90% highest posterior density intervals (HPDIs). We also report evidence ratios (ERs), which are equivalent to (one-sided) Bayes factors, to quantify the relative posterior probability for a directed effect compared to its alternative [30].

Foraging performance and scrounging

Participants incentivized on the group level showed no difference in performance between environments (-0.05 [-8.9,8.1], ER = 1.05; Fig. 2a; Supplementary Table 1), whereas participants incentivized on the individual level performed worse in concentrated than distributed environments (-8.4 [-16.7, -0.5], ER = 20.7). To quantify success differences among incentive conditions over time, we computed exploitation probabilities at one minute intervals in each round (Fig. 2b; Supplementary Fig. 1). In concentrated environments, group-incentivized participants consistently outperformed those incentivized on the individual level after four minutes. In distributed environments, individually-incentivized participants initially performed better before converging on the same probability of success. Investigating success conditional on prior experience (Supplementary Table 2), we found that group-incentivized participants performed substantially better than individually-incentivized participants when foraging in concentrated environments for a second consecutive time (15.0 [4.3, 26.2], ER = 76.7), but not in the first round of the experiment (3.1 [-8.6, 14.3], ER = 2.1) or when having previously foraged in distributed environments (0.01 [-11.3, 11.4], ER = 0.99).

The structure of the environment also induced different patterns of foraging behavior. In concentrated environments, participants discovered fewer new patches (group incentives: -5.2 [-5.7,-4.7], ER > 100; individual incentives: -5.6 [-6.1,-5.1], ER > 100; Supplementary Table 3) but joined more patches discovered by others (group incentives: 1.4 [0.7,2], ER > 100; individual incentives: 1.1 [0.4,1.8], ER > 100; Supplementary Table 4). Participants also stayed closer to group members (average distance to the other three players when focal player was not exploiting; group incentives: -6.4 [-7.6, -5.3], ER > 100; individual incentives: -8.8 [-10.1, -7.6], ER > 100; Supplementary Table 5) and looked more at others (average number of players in field of view when focal player was not exploiting; group incentives:

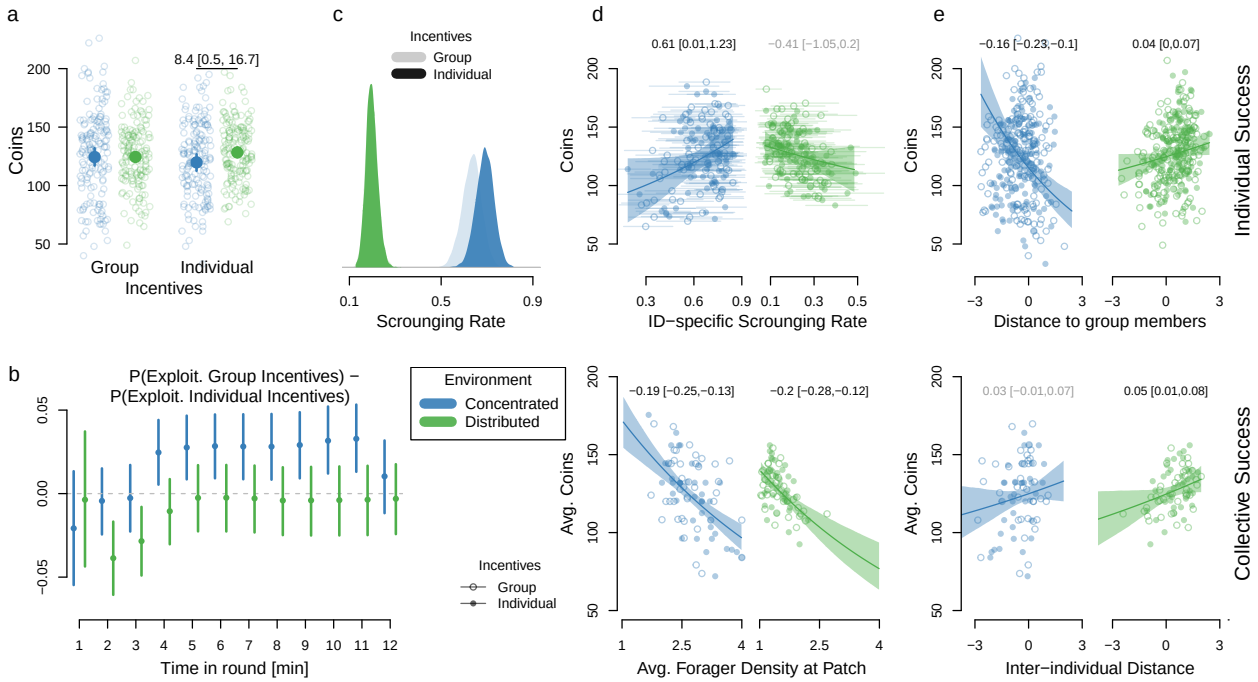

Fig. 2: **Behavioral Results**. (a) Coins collected per incentive condition and environment. Each circle represents one round per participant, larger filled dots represent posterior estimates (as well as 90% HPDIs) from a Bayesian multilevel Poisson model. (b) Performance differences between incentive conditions (positive values indicate an advantage for group incentives), computed as the probability of exploiting a patch in one minute intervals. (c) Posterior scrounging rates (conditional probabilities that players join a patch where they had observed at least one exploiting group member) per incentive condition and environment. (d) Average number of coins collected per individual as a function of individual-specific scrounging rates (with 90% HPDIs; top) and per group as a function of forager density (i.e., average number of players exploiting a given patch; bottom). (e) (Average) number of coins per round per individual (top) and group (bottom) in concentrated and distributed environments as a function of distance (standardized average distance to other players). Lines and uncertainty intervals show effects from multilevel regressions accounting for baseline differences between incentive conditions and individual- and group-level variability in both intercepts and slopes (transparent text if 90% HPDI overlaps 0).

0.08 [0.05,0.1], ER > 100; individual incentives: 0.14 [0.11,0.17], ER > 100; see Supplementary Fig. 2; Supplementary Table 6), suggesting increased social attention in concentrated environments (see Supplementary Fig. 3 for aggregated results).

To account for the influence of participants' unique visual perspectives, we next computed scrounging rates as conditional probabilities for players to join a patch where they had observed one (or more) exploiting group member(s). Scrounging rates were higher in concentrated than in distributed environments (group incentives: 0.44 [0.37,0.50], ER > 100; individual incentives: 0.48 [0.42,0.54], ER > 100), with most scrounging behavior seeming to occur in participants incentivized on the individual level while foraging in concentrated environments (individual vs. group incentives in concentrated environments: 0.06 [-0.03,0.16], ER = 5.7; Fig. 2c; Supplementary Table 7).

Determinants of individual and collective success

Can this apparently excessive scrounging explain the reduced performance of individually-incentivized participants in concentrated environments? To relate behavioral metrics to the number of collected coins, we used multilevel Poisson regressions accounting for baseline success differences between incentive conditions. In concentrated environments, individual participants benefited from high scrounging rates (Fig. 2d, top) and close proximity to others (Fig. 2e, top). This confirms individual-level adaptive benefits of social information use in resource environments where the behavior of others provides valuable information. By contrast, collective performance was higher if, on average, fewer players exploited a patch (Fig. 2d, bottom) and, to a lesser degree, if group members kept greater inter-individual distance (Fig. 2e, bottom), revealing opposing effects of social information use on individual vs. collective performance. In distributed environments, where social information has lower value, both individual and collective performance was highest if partici-

pants joined fewer patches discovered by group members and stayed further away from each other.

Beyond social information use, participants also collected more coins if they independently discovered more new patches in both concentrated (0.14 [0.12,0.15], ER > 100) and distributed (0.09 [0.08,0.09], ER > 100) environments as patch discoverers had more time to collect coins without sharing resources with others. For both environments, participants with relatively directed and regular movement trajectories discovered more patches highlighting an important role for effective individual search (Supplementary Fig. 4).

Solitary foragers

To compare group foragers to solitary ones, we recruited additional participants who searched for coins on their own (see Methods). Foraging in the same resource environments but without competition, individual foragers, on average, collected more coins than participants in groups. They performed similarly in both environments and discovered more patches in distributed environments (Supplementary Fig. 5; see Supplementary Fig. 6 for movement metrics and discoveries).

Social Hidden Markov Decision Model

Next, we use a computational approach to delineate the mechanisms underlying participants' decisions to respond to or ignore social information. A computational approach is necessary because observable metrics, such as patch joining events, are only indirect indicators of underlying strategies [31]. Such latent strategies as well as the decisions to switch between them lie at the core of theoretical (producer-scrounger) models but cannot be directly observed. Imagine, for instance, that a player decides to use social information and moves towards an exploiting group member but does not arrive before all coins are collected; or, more luckily, this player might even independently discover a new patch while relocating. In both scenarios, we do not observe the player joining a patch, although they have actively decided to use social information.

Our model uses time series of three state-dependent variables (on a one-second resolution; Fig.1d and Supplementary Fig. 7) to probabilistically assign participants to one of two latent states at each point in time: *individual exploration* or *social relocation* (see Methods). Individual exploration is characterized by irregular movement not directed towards successful peers, whereas social relocation is characterized by consistent, directed movement towards exploiting group members. Note that the latent states are statistically inferred from changes in movement and interaction patterns, not hard-coded based on arbitrary criteria; we only selected the number of latent states and provided the model with prior information about how the states are expected to differ (i.e., which state should have larger values in the state-dependent variables). Reassuringly, the model estimated smaller turning angles, larger reduction in distance to exploiting players and smaller relative bearings for the social relocation state compared to the individual exploration state (Supplementary Fig. 8), confirming that the identified latent states correspond to our target of inference (Supplementary Fig. 7 shows an example of a recovered state sequence using the Viterbi algorithm).

State predictors and their adaptive consequences

Our model simultaneously infers the time-dependent transition probabilities between latent states. This allows us to describe how incentive conditions i and resource distributions j along with currently available (visual) information influence the probability of switching from individual exploration to social relocation at time t. Specifically, we estimated the condition-specific influence of exploitation visibility V, visible patch distance D, number of visible exploiting players N, and time since success T (Fig. 1d; see Methods) :

$$P_{I->S_t} = logit^{-1}(\alpha_{i_{j_{[t]}}} + \beta_{V_{i_{j_{[t]}}}} V_t + \beta_{D_{i_{j_{[t]}}}} V_t D_t + \beta_{N_{i_{j_{[t]}}}} V_t N_t + \beta_{T_{i_{j_{[t]}}}} T_t). \quad (1)$$

Averaging over all situations when at least one exploiting player was visible (i.e., $V = 1$), participants were more likely to switch to social relocation and approach others in concentrated compared to distributed environments with both group (0.03 [0.004, 0.06], ER = 26.4) and individual (0.05 [0.02, 0.08], ER > 100) incentives (Fig. 3a, first row). Moreover, individual incentives reliably increased participants' propensity to use social information in concentrated (0.04 [0.002, 0.07], ER = 21.7) but less so in distributed (0.01 [-0.01, 0.04], ER = 5.8) environments. Thus, participants were more likely to switch to social relocation when prioritizing their individual success, particularly in concentrated environments where scrounging is beneficial, uncovering the decision mechanisms underlying the observed scrounging rates (Fig. 2c). Using individual decision-weight estimates (i.e., random effects of state predictors from the multilevel computational model) to predict success reveals that individuals benefited from more social information use in both environments (Fig. 3b, first row).

Turning to the strategies participants used to integrate social information, we found that, across conditions, participants were more likely to use social information if observed successful group members were close rather than farther away, suggesting selective rather than indiscriminate use of social information (Fig. 3a, second row). This selectivity with respect to distance proved adaptive in distributed, but not in concentrated environments (Fig. 3b, second row). Moreover, participants preferentially decided to join patches where fewer group members were exploiting in the

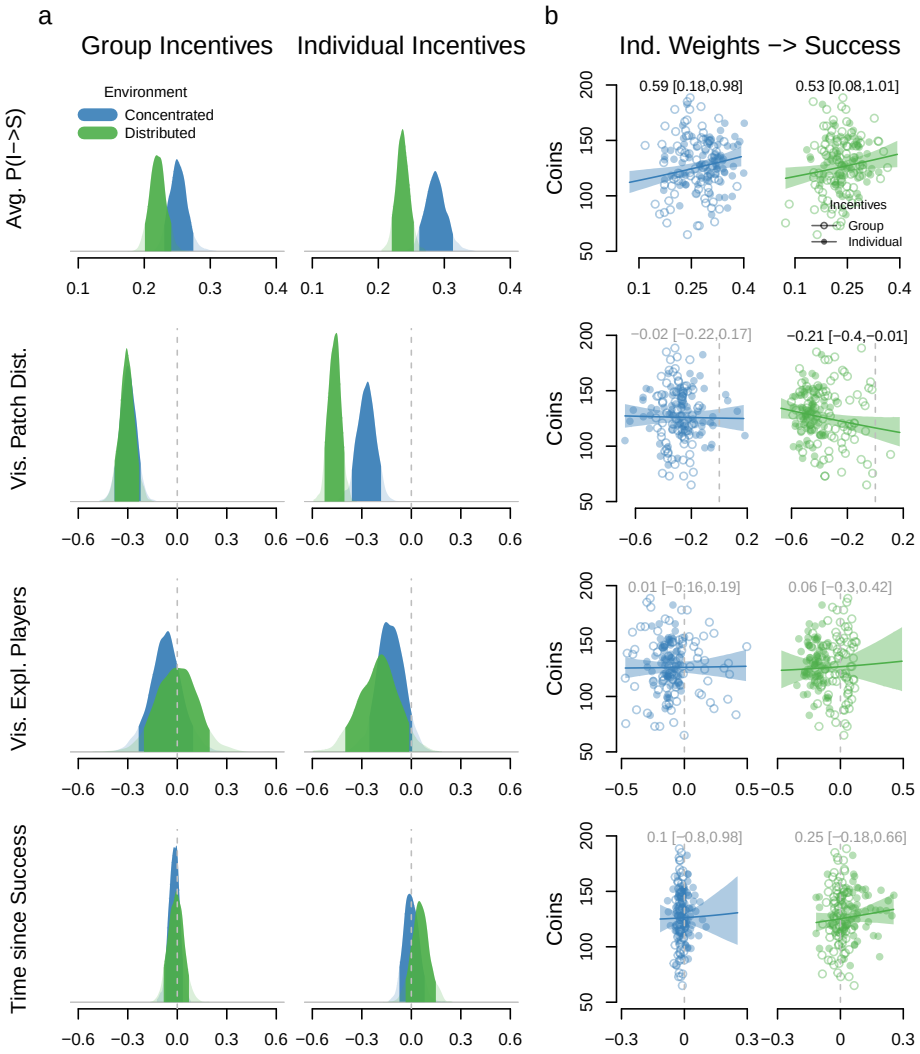

Fig. 3: **State predictors and their adaptive consequences** (a) Full posterior distributions (transparent curves) and 90% HPDIs (darker areas) for the influence of different state predictors on the probability that participants switch from individual exploration to social relocation per environment and incentive condition. The top row shows baseline switching probabilities across all situations in which participants observe (a) successful player(s), the other rows show deviations from this expectation on the logit scale. (b) Success (average number of coins collected per individual) in concentrated (left) and distributed (right) environments as a function of individual-level decision weights. Lines and uncertainty intervals show effects from log-normal regression models accounting for baseline success differences between incentive conditions (reported above, transparent text if 90% HPDI overlaps 0).

individual but not in the group incentive condition (Fig. 3a, third row). Being selective with respect to the number of others at a patch proved neutral in both environments (Fig. 3b, third row), likely reflecting the fact that participants observed two players exploiting the same patch in only 14% of cases and three players in only 3% of cases (one player in 83%). As a last factor, we also investigated the influence of past personal success on the probability to respond to social information. Surprisingly, we found that participants did not become more likely to use social information if unsuccessful for a longer time and there was also no relationship between individual-level weights and foraging success (Fig. 3a,b, fourth row).

Investigating the role of latent decision weights on collective performance confirms the same pattern observed for behavioral outcomes (Supplementary Fig. 9). The average baseline probability to turn social for groups was negatively related to collective success in concentrated environments, again revealing a striking contrast to individual-level outcomes where high social information use proved beneficial. Other decision weights were unrelated to collective success.

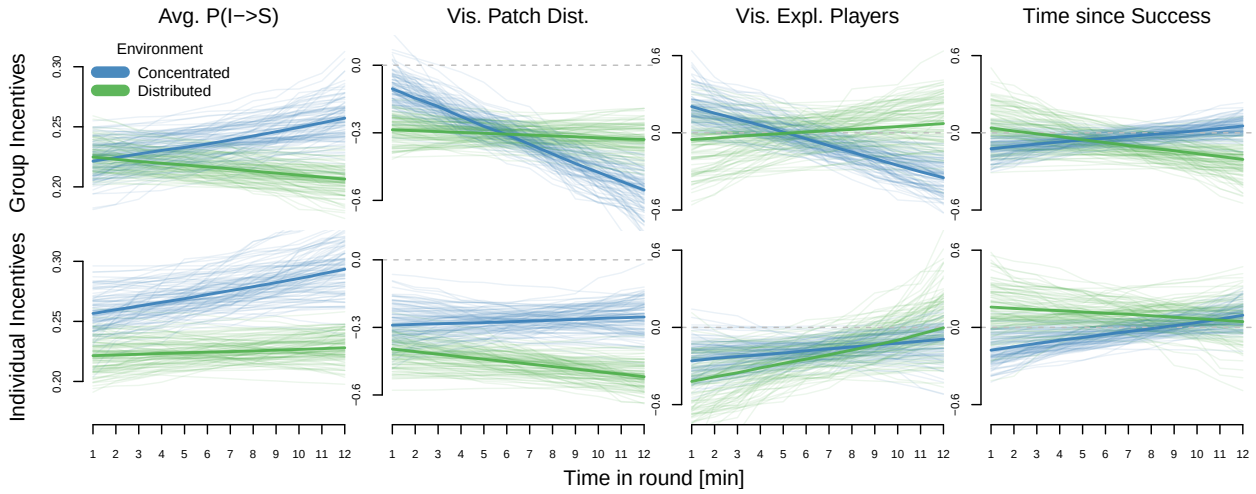

Fig. 4: **Temporal dynamics in state predictors.** 100 random draws from the posterior distribution (transparent lines) as well as posterior means (solid lines) for the influence of different state predictors over time in each round. The first column shows baseline switching probabilities across all situations in which participants observe (a) successful player(s), the following columns show deviations from this expectation on the logit scale.

Temporal dynamics in state predictors

Over time, group-incentivized participants outperformed those incentivized on the individual level in concentrated environments (Fig. 2b; Supplementary Table 2). Did participants adjust their decision-making over time or did they enter the experiment with fixed, unchanging strategies? Figure 4 shows the temporal dynamics in state predictors from the time-varying state predictors model (see Supplementary Fig. 10 for similar linear trends).

We first focus on participants incentivized on the group level. Participants started with similar overall propensities for social information use in both environments but, over time, seemed to become more likely to use social information in concentrated (0.20 [-0.01, 0.42], ER = 12.8) and less likely to use social information in distributed environments (-0.11 [-0.27, 0.05], ER = 6.2), suggesting calibration of social decision-making over time. Participants in concentrated environments started as rather indiscriminate social learners but, over time, became more selective and began to strongly rely on distance (-0.45 [-0.64, -0.26], ER > 100) and the number of exploiting players (-0.55 [-0.88, -0.24], ER > 100) as cues. This tuning of decision strategies towards more selectivity might act as a safeguard against the over-reliance on social information and, therefore, (partly) explain the emerging benefits of collectively-incentivized participants (Fig. 2b). In distributed environments, decision weights stayed relatively constant and there were no clear trends in the influence of the time since the last success.

In the individual incentive condition, baseline levels of social information use started at higher levels compared to the group incentive condition and seemed to increase even further in concentrated environments (0.18 [-0.03, 0.40], ER = 10.4). Unlike collectively-incentivized participants, there was no distinct development towards more selective social information use in either environment.

Collective visual-spatial dynamics

Our behavioral results suggested that, averaging over the whole rounds, groups benefited from less social information use and lower proximity in both environments (Fig. 2d,e, bottom). However, collective outcomes dynamically unfold over time, calling for a deeper understanding of the timescales at which the costs and benefits of social information use occur. To examine such fine-grained collective dynamics, we quantify the changing relationships between groups' visual-spatial organization and collective foraging success for different time lags (Fig. 5; Supplementary Fig. 11 shows results for up to 3-minute time lags in steps of 5 seconds). Positive (negative) regression weights for a given time lag τ mean that greater inter-individual distance/visibility among group members at time $t - \tau$ increased (decreased) groups' current collective foraging success at time t.

In distributed environments, groups of individuals who stayed farther away from each other were indeed more successful irrespective of time interval and incentive condition. In concentrated environments, we observed more intricate temporal dynamics. At relatively short timescales ($<\approx 15s$ for group incentives, $<\approx 8s$ for individual incentives), smaller inter-individual distances were associated with greater collective success; being closer together allowed collectives to better exploit clustered resources discovered by group members.

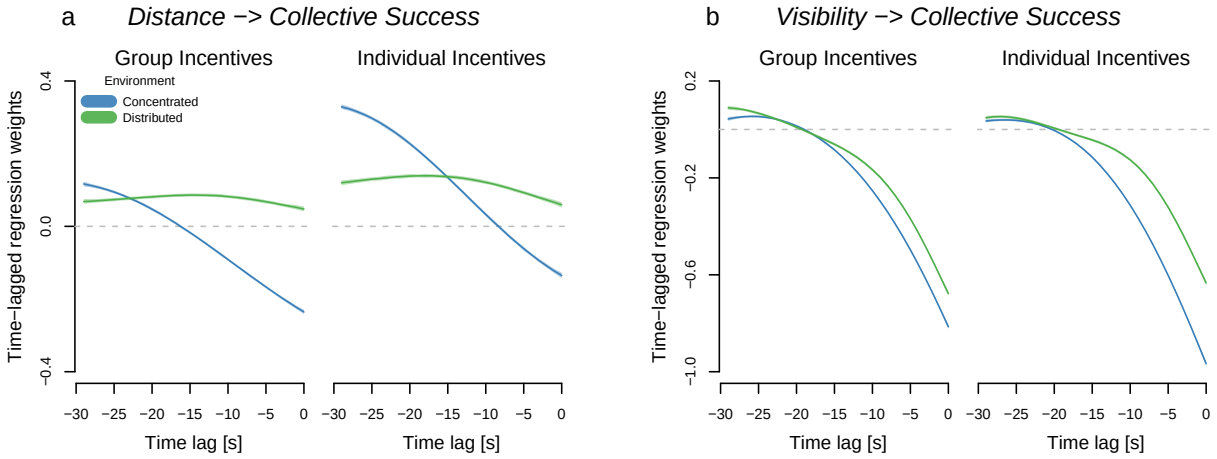

Fig. 5: **Collective visual-spatial dynamics**. Time-lagged Gaussian-process regression weights (including 90% HPDIs) predicting collective foraging success (number of players exploiting a patch) based on (a) distance (average pairwise distance among players) and (b) visibility (number of visual connections among group members, ranging from 0, where no one is looking at others, and 12, where everyone is looking at everyone else) across different time intervals per incentive condition and environment.

This beneficial effect of grouping was especially pronounced for groups incentivized on the collective level. On the flip side, at longer timescales, larger distances among group members were associated with greater foraging success. If groups disperse, they are better able to explore large parts of the environment and discover one of the few, rich patches, thereby, increasing their collective foraging success in the future. Individually-incentivized groups benefited more strongly from spatial distancing, likely because their higher sensitivity to social information increased their risks for over-exploitation and herding. At even longer timescales, there was no longer an association between group distance and foraging success (Supplementary Fig. 11).

Turning to inter-individual visibility, we observe a strong negative effect at short timescales ($<\approx 20s$) for both environments and incentive conditions. As players could not see others while exploiting a patch, low visibility often meant that a lot of players were currently collecting coins. More substantially, the number of visual connections among group members was positively related to collective success longer into the future across all conditions, suggesting that groups paying more attention to others in this crucial time window of patch discovery had greater success later on.

3. Discussion

Finding and collecting rewards in heterogeneous environments is key for adaptive collective behavior, yet it remains largely unknown how individuals in freely interacting groups make strategic choices in naturalistic environments and how these choices might shape individual and collective outcomes. We designed a 3D immersive-reality collective foraging paradigm to obtain fine-grained visual and spatial data from interacting groups and developed computational Social Hidden Markov Decision models to extract and understand strategic choices from naturalistic behavior. Collective foraging provides an ideal testbed to study social decision-making and collective adaptation in a controlled, yet ecologically-relevant, context [1, 32]. Anthropologists have identified our unique abilities to collectively find and extract high-quality resources from diverse environments as a defining feature of human adaptability [33–36]. Collective foraging further unites several key ecological and social challenges, such as navigating uncertain environments, cooperating with others to achieve common goals, as well as competing to gain privileged access to resources [32, 37].

As predicted by game-theoretic models of collective foraging [e.g., 10, 25, 38], participants systematically adjusted their social information use to the resource distribution relying more on the behavior of others when resources were difficult to find, but provided a large potential for exploitation (i.e., in concentrated compared to distributed environments). Our work not only translates and tests predictions from idealized producer-scrounger models in more realistic social scenarios but, thereby, also highlights the fundamental role space and perception play in modulating social decision-making. Moreover, we found that participants calibrated their strategies over time, becoming more (less) likely to use social information in concentrated (distributed) environments, extending previous research highlighting the importance of selective and strategic social learning rather than pure copying or innovation [13, 15, 20].

In both environments, individuals benefited from high propensities to switch to social relocation, whereas actually capitalizing on social information and scrounging at patches discovered by others was only adap-

tive in concentrated environments but maladaptive in distributed environments. The reason for this apparent contradiction might be that participants could still discover new patches while approaching group members and more directed movement even generally increased their chances of patch discovery. Therefore, participants incurred little costs by frequently responding to social information even if resources were evenly distributed, thus generating divergent consequences for latent propensities to respond to social information compared to manifest outcomes. Moreover, in distributed environments, where far-away patches were likely depleted before arrival, participants collected more points if they tuned their propensity to switch to social relocation based on the distance of exploiting group members, confirming recent theoretical predictions on the importance of selective copying in collective search [39].

Large amounts of social information use proved adaptive for individuals (in concentrated environments) but maladaptive for collectives. Groups performed better in either environment if, on average, fewer players exploited a given patch and players stayed further away from each other; additionally, solitary foragers generally outperformed participants in groups. Crucially, placing the incentives on the collective level alleviated the negative collective consequences of high social information use. In concentrated environments, where scrounging is individually beneficial, collectively-incentivized participants were less likely to respond to social information and exploit patches discovered by others, increasing their foraging success compared to participants incentivized on the individual level. Group incentives had a more reliable effect on latent switching probabilities compared to observed scrounging rates. This is likely because switching probabilities in the computational model directly reflect decisions to use social information and approach successful others, whereas scrounging rates are influenced by many other factors beyond an individual's control such as the behavior of others, highlighting the need to model social information use at the level of latent decisions instead of noisy behavioral outcomes. Moreover, group incentives also facilitated adaptive tuning of latent decision strategies over time, with increased selectivity likely safeguarding against maladaptive over-use of social information. There was no change towards more selective social information use in the individual incentive condition, suggesting that participants consistently aimed to maximize their own success which benefited from frequent scrounging. Previously, Hung and Plott showed that a "majority rule institution" where participants were rewarded depending on group accuracy, reduced information cascades [40]. Similarly, Bazazi and colleagues showed that collective incentives reduced individuals' reliance on social information in an interactive group estimation task and, thereby, increased the diversity of opinions and group wisdom [41]. The present findings extend such work demonstrating how incentive structure together with environmental affordances influence social information use and its collective consequences in more unconstrained and spatially explicit scenarios.

At first glance, the collective drawbacks of high social information use we observed seem to contradict models of collective search [e.g., 38, 39, 42] that have shown that high degrees of social information use can also be beneficial on a collective level in rich and clustered environments. However, in such models, individual exploration is typically governed by a random walk or similar stochastic process and social information provides the only source of adaptive information. Human participants, in contrast, use rich internal models of the environment and the task, as well as memory, to systematically search the arena. These enhanced individual exploration abilities likely shifted the relative collective benefits of personal and social information use compared to theoretical models. Moreover, our time-lagged dynamics analysis provided a subtler picture of when and how it was beneficial for collectives to join forces. In distributed environments, collectives indeed consistently benefited from independent search. In concentrated environments, close spatial proximity allowed groups to efficiently exploit discovered patches, while, at longer timescales, collectives benefited from larger distances, facilitating new patch discoveries and increasing foraging success in the future. Therefore, if resources are rich but hard to find, collective foragers need to dynamically adjust their visual-spatial organization over time and collectively strike the right balance between independent exploration and joint exploitation.

A promising avenue for future research could be to investigate cases of collective foraging where social information use does not create zero-sum scenarios as in the present paradigm but facilitates novel adaptive abilities to emerge on the group level such as collective tracking of mobile resources [43–45]. Other interesting extensions of the present paradigm would be to systematically vary group size, which has been predicted to affect the rate of scrounging [25], and to include patches of different qualities forcing individuals to additionally decide when to leave a given patch [46]. As we found that the benefits of collective incentives increased over time (both within and across rounds), researchers could also investigate in greater detail how individuals (and collectives) update their strategies as a function of their own and observed payoffs.

Moving forward, we want to emphasize that developing more naturalistic experimental paradigms should not be a research goal in itself, unless the added complexity provides additional theoretical insights. By "naturalistic", we thus do not mean conditions that are simply more complex or appear more similar to the real world, but heterogeneous environments which are shaped endogenously as a consequence of one's own and others' actions and which are marked by temporal and spatial autocorrelation [47, 48]. In our case, including perceptual and spatial constraints added key features of real-world decision environments [21, 25],

which, as we showed, fundamentally shape the costs and benefits of social information use. The cues that participants can base their decisions on (e.g., the distance to visible others) arise naturally as a consequence of their choices and the behavior of others instead of being externally imposed by the experimenter. As the ecological validity of such cues (i.e., the degree to which they reflect statistical patterns in the world) also determines the ecological validity of the experiment itself [49], naturalistic approaches in this stricter sense also help us to bridge the gap between the lab and the real world.

Finally, to identify and model latent choices between different behavioral states ("Individual Exploration" and "Social Relocation"), we developed a novel Social Hidden Markov Decision model. Traditionally, cognitive and behavioral scientists have investigated choices in relatively static and highly standardized experimental situations. Although abstracting away from real-world details and controlling the environment participants face can allow researchers to more accurately identify cognitive processes and strategies, ultimately, we aim to understand how people make unconstrained decisions in relevant real-world ecologies. Technological advances now provide us with unprecedented access to the individual-level informational environments and constraints that guide strategic choices in humans and other animals [20, 50, 51]. Such dynamic data require dynamic statistical inference and Hidden Markov models provide ideal tools to simultaneously extract meaningful patterns from multidimensional time-series data and use internal or external situational factors to predict switches between the identified hidden states. Although our model is tailored to the present experimental paradigm (especially with respect to the state-dependent variables), our freely available modeling code and in-depth documentation set the scene for future research on the socioecological drivers of social decision-making in human and (non-human) animal collectives. In addition to other naturalistic behavioral experiments [20, 52, 53], Social Hidden Markov Decision models can, for instance, be applied to human crowd behavior to better understand how situational factors influence movement patterns and potentially cause stampedes [54, 55]; they can be adapted to sports analytics where Hidden Markov models have already been used to identify drive events and defensive assignments in basketball [56, 57] or "hot hands" in darts [58]; they could elucidate dynamic leader-follower dynamics in animal societies and help us better understand when and why animals follow the example of others [59, 60]; and they could be applied to GPS data from subsistence foragers [61, 62], cell phone users [63, 64] or migratory animals [65–67] to infer modes of (collective) search, movement and space use across different spatial and temporal scales.

In summary, our work mechanistically links individual-level social information use to collective dynamics in naturalistic interactions. Through behavioral and computational analyses, we have demonstrated how group incentives can improve collective performance by reducing individually beneficial, but collectively costly, exploitation of social information. Maybe most importantly, this work showcases a novel way of studying human behavior that goes beyond the often highly constrained experiments of psychology, economics, and cognitive science, moving towards a science of unconstrained behavior that dynamically unfolds in naturalistic and socially interactive environments.

4. Methods

Participants

160 participants were recruited from the Max Planck Institute for Human Development (MPIB) recruitment pool and invited in anonymous groups of four to the behavioral laboratory at the MPIB in Berlin, Germany (63 identified as male, 97 as female; $M_{\text{age}} = 28.5$, $SD_{\text{age}} = 6.4$ years; all were proficient in German and most came from Western, educated, industrialized, rich, and democratic societies [68, 69]). 40 additional participants were recruited for an individual control condition (14 identified as male, 26 as female; $M_{\text{age}} = 29.8$, $SD_{\text{age}} = 5.7$ years). The study was approved by the Institutional Review Board of the MPIB (number: A 2022-06) and participants signed an informed consent form prior to participation. Participants received a base payment of €18 plus a bonus of €0.01 per coin (depending on incentive condition, see below), earning on average €23.09 ± 0.71 (SD) for a total time of about one hour.

Procedure

Participants started with an in-game tutorial to familiarize themselves with the keys and virtual environment (see Supplementary Video 2). Participants then completed the task in groups of four, interacting live in a 3D immersive game environment. Group members were seated in the same room; opaque desk divider panels ensured that they could not observe each other's screen and mice with silent buttons prevented them from hearing when others clicked on coins during the coin collection mini-game. Over four rounds lasting twelve minutes each, participants controlled avatars in the virtual world (a square 90m x 90m "castle courtyard") and searched for resources ("coins") hidden under ground (Fig. 1a; Supplementary Video 1). At the beginning of each round, a fixed number (see section below) of non-overlapping circular resource patches ("coin fields") with a radius of $r = 3$ meters was randomly placed across the arena. Participants used keyboard buttons to freely navigate through the virtual environment and detect resource patches with a metal detector. Participants could only move their avatar forward, turn right or turn left using the "W","A" and "D" keys, respectively. All other keys were deactivated.

When individuals encountered a patch, their metal detector lighted up and they could start collecting coins by clicking on coin symbols appearing at different locations on the screen (Fig. 1b). New coins appeared at a fixed interval of two seconds and stayed on the screen until collected (this interval was chosen as pilots showed that all participants were able to collect coins within two seconds). This simple "mini game" ensured that participants stayed engaged throughout the ex-

periment without introducing additional sources of variation in performance. Participants continued collecting coins at a patch (and, therefore, could not move) until it was depleted. After that, the patch disappeared and a new patch containing the same number of coins was generated at a random location in the environment (ensuring that it did not overlap with any existing patch or participant). This means the number of patches and, therefore, the task structure remained constant within each round avoiding any effects of resource depletion or diminishing returns.

In addition to individual exploration of the environment, participants could also observe the behavior of others and freely decide to join players who have successfully discovered a resource patch. Avatars in the virtual environment performed a digging movement using a shovel to indicate that they were currently extracting coins (right avatar in Fig. 1a). If multiple players simultaneously collected coins from the same patch, each player extracted coins at the same rate of one coin every two seconds and coins, therefore, disappeared from a patch at a rate proportional to the number of extracting players. This means there was exploitative, but not interference, competition among players. Participants were only informed about the total number of coins collected (individually or collectively, depending on condition) after each round, but did not receive any additional feedback during rounds.

The 3D virtual environment imposed a limited, first-person, field of view (108° horizontal and 76° vertical FOV) as well as realistic spatial constraints (maximum movement speed of 2 m/s) creating natural trade-offs between individual exploration of the environment and social information use [20, 22]. The experiment was implemented using the *Unity* [70] game engine (version 2020.3.21 [71], built-in rendering pipeline) with the Netcode for GameObjects and Unity Transport libraries for networking functionality. The four instances for participants were connected to a local Windows Server running a Server Build of the experiment with a tick rate of 25Hz. Player movement was handled client-side. The Unity source code as well as built executives necessary to reproduce and run the experiment are stored on GitHub: https://github.com/DominikDeffner/VirtualCollectiveForaging.

Experimental Design

The experiment followed a 2x2 design (Fig. 1c). Groups of participants were either incentivized on the individual or group level (between-subjects factor). In the "Individual Incentives" condition, participants' reward payment depended solely on their own amount of coins collected. In the "Group Incentives" condition, participants were rewarded based on the average number of coins collected across all four group members. As a second (within-subjects) factor, we manipulated the resource distribution: The same number of coin resources was either concentrated in few but rich patches ("Concentrated" condition; 5 patches with 48 coins each) or distributed among many but poor patches ("Distributed" condition; 15 patches with 16 coins each). Participants experienced each resource distribution twice and all possible permutations of presentation order were realized for both incentive conditions. The resource distribution for each round was announced prior to the start of each round and was also indicated by the color of the walls enclosing the arena. Participants in the individual foraging condition searched for coins on their own with the same resource distributions and were paid depending on the number of coins collected.

Data

At a sampling interval of 25Hz, we recorded participants' (1) X- and Y-coordinates, (2) orientation vector, (3) velocity, (4) coin count and (5) whether they were extracting or not. From this raw data, we constructed movement trajectories of all players and computed the full visual social information available at each point in time through basic triangulation (Supplementary Video 3; see GitHub repository for complete data-processing scripts: https://github.com/DominikDeffner/VirtualCollectiveForaging). Moreover, we recorded (1) when a player arrived at a patch, (2) when a player extracted a coin, (3) when a patch was depleted, and (4) when and where a new patch was generated. For each event involving a player, we recorded the time stamp and ID of the player.

Behavioral analyses

Temporal dynamics of success

To quantify how participants' performance changes over time, we used a multilevel model with Bernoulli likelihood to predict whether players are currently exploiting a patch on a one-second resolution. In addition to intercepts for each experimental condition and individual- and group-specific offsets, we used time (minute in round) as an ordered categorical (or monotonic) predictor, which also varied by condition. Instead of imposing a particular functional form (e.g., a line), this approach only assumes that performance changes monotonically over time (i.e. either constantly increases or decreases) and lets the model estimate the size of the steps in which success probabilities change [15, 72]:

$$P(E)_{ij}^{\tilde{t}} = logit^{-1}(\alpha_{ij} + \beta_{ij}^{MAX} \sum_{m=0}^{\tilde{t}-1} \delta_{ij}^{m}). \quad (2)$$

The probability that players are exploiting in a specific minute of a round, indicated by $\tilde{t}$, is composed of the intercept for each incentive condition i and environment j and the total effect of experimental time multiplied by a sum of δ-parameters which represent the additional effect of each increment in time (all δs together sum to 1).

Scrounging analysis

To infer behavioral scrounging rates, we computed conditional probabilities for players to join a patch where they observed at least one exploiting group member. We first computed at which patches players observed an exploiting group member and then modeled the proportion of those patches that players actually joined using a binomial likelihood function. In addition to condition-specific intercepts, we implemented individual- and group-level random effects. This also allowed us to use estimated individual-level scrounging rates (compared to other group members) to predict success in both environments within the same model propagating the full range of uncertainty (Fig. 2d; top).

Social Hidden Markov Decision Model

We used a computational approach to study how different social and asocial cues impact participants' decisions to use social information and switch between behavioral states across

the different conditions. Inspired by tools and concepts from animal movement ecology [28, 29, 73], we developed a novel Social Hidden Markov Decision Model. A Hidden Markov model is a doubly-stochastic time-series model with an observation process and an underlying state process (Fig. 1d). It resembles a finite mixture model with several outcome variables where the identity of the underlying distributions is controlled by a Markov chain [74]. The model uses time series of "state-dependent variables" (on a one-second resolution) to probabilistically assign each time point per participant to one of a fixed number of latent behavioral states. Participants can be in three different states: individual exploration, social relocation and exploitation [75]. Since exploitation is observed, our only hidden states are individual exploration and social relocation and the model estimates parameters of the distributions that characterize both states. Additionally, our Social Hidden Markov Decision Model simultaneously infers the transition probabilities between both latent behavioral states and we included time-dependent (social and asocial) "state predictors" that influence such transitions.

State-dependent Variables

We used three state-dependent variables to infer the latent states from the data: (1) participants' turning angles (change in movement direction in radians between successive time points; social relocation is expected to be characterized by directed movement, i.e., small turning angles), (2) the (smallest) change in distance to visible exploiting player(s) (social relocation marked by large reduction in distance to observed exploiting players) and (3) the (smallest) relative bearing (angle between orientation vector and vector connecting focal player to each other player; social relocation marked by consistent orientation towards other player, i.e., small relative bearing). Supplementary Fig. 7, top three rows, illustrates the state-dependent variables for one exemplary time series with orange bars representing periods identified by the model as social information use through the Viterbi algorithm [76, 77]. To model the turning angles, we used the von Mises distribution which is commonly used in directional statistics for continuous circular data. It is a (more tractable) close approximation of the Wrapped normal distribution [78]. For change in distance and relative bearings, we used normal and log-normal likelihoods, respectively.

State Predictors

To quantify how experimental conditions and situational factors modify each participant's probability to stop exploring independently and switch to social relocation at each time point t, we used four state predictors (Supplementary Fig. 7, bottom four rows): (1) a binary visibility indicator ($V = 1$ if any exploiting player is currently in field of view, $V = 0$ otherwise), (2) the (z-standardized) distance to the closest *visible* exploiting player D, (3) the number of other players extracting at the closest *visible* patch N (coded such that $N = 0$ represents the default where only one player is exploiting) and (4) the (z-standardized) time since the last coin extraction T. All state predictors were estimated for each incentive condition i and environment j (Eq. 1). Note that D_t and N_t are multiplied by V_t in Eq. 1 to "switch on" the effects of distance and player number only for times when participants actually observed (an) exploiting player(s), i.e., when $V_t = 1$. All predictor weights were estimated in a fully hierarchical Bayesian framework with random-effect terms accounting for the covariance of decision weights among both individuals and groups while also allowing those covariances to differ among experimental conditions (omitted from Eq. 1 for the sake of readability).

Time-varying state predictors

Moreover, we augmented these multilevel models by estimating time-varying parameters through ordered categorical (monotonic) effects and describe how social decision-making dynamics unfold over time. As one example (other state predictors are constructed equivalently), the effect of patch distance on the probability to switch to social relocation in a specific minute of a round $\tilde{t}$ is composed of the total effect of time times the sum of δ-parameters which represent the additional effect of each increment in time:

$$\beta^{\tilde{t}}_{D_{ij}} = \beta_{D^{MAX}_{ij}} \sum_{m=0}^{\tilde{t}-1} \delta_{D^{m}_{ij}}. \quad (3)$$

Note we only included individual- and group-specific offsets for the average effect of each state predictor over time.

Forward and Viterbi algorithms

To efficiently compute the (log) marginal likelihood, i.e., the joint distribution of each data sequence summing over all possible state sequences, we used the *forward algorithm*, which calculates this likelihood recursively [see 28, 73, 74, 76, for more technical introductions]. After model fitting, we used the dynamic-programming *Viterbi algorithm* to obtain the most likely state sequence given the observations and estimated parameters [28, 74, 76]. This reconstruction of the underlying state sequence helps visualizing the results of the fitted models and ensuring that the state-dependent distributions can be connected to psychologically meaningful processes. We only explicitly modeled times at which players potentially could use social information, i.e., times when they were allowed to move and at least one group member was currently collecting coins (white segments in Supplementary Fig. 7). This means we omitted all times (1) when players themselves were exploiting a patch (dark grey segments in Supplementary Fig. 7) and (2) when no group member was exploiting (light grey segments in Supplementary Fig. 7), because in both cases we know the state of a player. To ensure a proper latent state sequence, we set a player's state to individual exploration after both types of omissions.

As detailed in the preregistration (https://osf.io/5r736/), we have developed a tailored collective foraging agent-based model combining individual-level evidence accumulation of personal and social cues with particle-based movement. We used this mechanistic model to generate synthetic data of the same format as our experimental data with known sequences of latent states (individual exploration and social relocation). We then confirmed that a baseline version of our computational model was able to reliably infer latent-state sequences on the level of single rounds.

Collective Visual-Spatial Dynamics Model

Lastly, we investigated how the visual-spatial organization of groups affected collective success across different timescales

and how these dynamics differed among incentive conditions and environments. Specifically, we used a time-lagged Gaussian-process regression model with binomial likelihood to estimate how spatial and visual organization at different times in the past $t-\tau$ (in steps of 5 seconds for up to three minutes, i.e., $t-5s, t-10s, ..., t-180s$, as well as for each second for up to half a minute, i.e., $t-1s, t-2s, ..., t-30s$) predicted collective success (proportion of players exploiting) at time t. Gaussian processes extend the multilevel approach to continuous categories and estimate a unique parameter value for each category, while still regarding time as a continuous dimension in which similar time lags are expected to generate similar estimates [72]. The regression weight for a given time lag $t-\tau$ (for incentive condition i and environment j) is composed of the average effect and a lag-specific offset for each experimental condition:

$$\beta_{ij}^{t-\tau} = \bar{\beta}_{ij} + d_{ij}^{\tau}. \quad (4)$$

The lag-specific offsets follow a multivariate Gaussian distribution, separately for experimental conditions:

$$\begin{pmatrix} d_{ij}^{1} \\ d_{ij}^{2} \\ ... \\ d_{ij}^{\tau_{max}} \end{pmatrix} \sim N\left[\begin{pmatrix} 0 \\ 0 \\ ... \\ 0 \end{pmatrix}, K_{ij}\right]. \quad (5)$$

The vector of means is all zeros, so the average effect remains unchanged, and K_{ij} is the covariance matrix among time lags. We estimated the parameters of a Radial basis function (or "squared-exponential") kernel that expresses how the covariance between different lags changes as the distance between them increases:

$$K_{ij}^{\tau_x \tau_y} = \eta_{ij} \exp(-\rho_{ij} \frac{(\tau_y - \tau_x)^2}{\tau_{max}^2}). \quad (6)$$

The covariance between time lags τ_x and τ_y equals the maximum covariance η_{ij}, which is reduced at rate ρ_{ij} by the relative squared distance between τ_x and τ_y.

Model fitting

All models were fitted using Stan as a Hamiltonian Monte Carlo engine for Bayesian inference [79], implemented in R v.4.0.3 through `cmdstanr` version 0.3.0.9 [80]. We used within-chain parallelization with `reduce_sum` to substantially reduce model run times through parallel evaluation of the likelihood. To reduce the risk of overfitting the data, we generally used weakly informative priors for all parameters. For state-dependent distributions in the Social Hidden Markov Decision Model, we used informative priors to incorporate knowledge about the nature of both states which also helps avoid label-switching, a common issue in all mixture models [28, 76]. To optimize convergence, we implemented the non-centered version of random effects using a Cholesky decomposition of the correlation matrix [72] with LKJ priors for correlations matrices [81]. Visual inspection of traceplots and rank histograms [82] suggested good model convergence and no other pathological chain behaviors, with convergence confirmed by the Gelman-Rubin criterion [83] $\hat{R} \leq 1.01$. All inferences are based on several hundred effective samples from the posterior [84]. Finally, we repeated our main behavioral analyses using frequentist methods and fitted generalized linear mixed models through `lme4` version 1.1-34. See GitHub repository for full model code and analysis scripts: https://github.com/DominikDeffner/VirtualCollectiveForaging.

Acknowledgements

We thank Jann Wäscher for recruiting participants, Philip Jakob for technical support, and Pietro Nickl for helping with Figure 1. This research has been supported by the Deutsche Forschungsgemeinschaft (DFG, German Research Foundation) under Germany's Excellence Strategy – EXC 2002/1 "Science of Intelligence" – project number 390523135. CMW is supported by the German Federal Ministry of Education and Research (BMBF): Tübingen AI Center, FKZ: 01IS18039A and funded by the Deutsche Forschungsgemeinschaft (DFG, German Research Foundation) under Germany's Excellence Strategy–EXC2064/1–390727645. The funders had no role in study design, data collection and analysis, decision to publish, or preparation of the manuscript.

Data and Code Availability

All relevant data and analysis code, the Unity source code as well as built executives necessary to reproduce and run the experiment are stored on GitHub: https://github.com/DominikDeffner/VirtualCollectiveForaging.

Author contributions statement

DD and RHJMK conceived the experiment, with feedback from DM, BK, CMW, and PR. DD, BK, and RHJMK performed the experiments. DD processed the data, analyzed the results and prepared the figures, with input from AS, CMW and RHJMK. DD wrote the first draft and all authors reviewed the manuscript.

Competing interests

The authors declare no competing interests.

References

1. Galesic M, *et al.*, 2023 Beyond collective intelligence: Collective adaptation. *Journal of the Royal Society Interface* **20**, 20220736
2. Tump AN, Deffner D, Pleskac T, Romanczuk P, Kurvers R, (in press) A cognitive computational approach to social and collective decision-making. *Perspectives on Psychological Science*
3. Krause J, Romanczuk P, Cracco E, Arlidge W, Nassauer A, Brass M, 2021 Collective rule-breaking. *Trends in Cognitive Sciences* **25**, 1082–1095
4. Wu CM, Dale R, Hawkins RD, 2023 Group coordination catalyzes individual and cultural intelligence. *PsyArXiv*
5. Giraldeau LA, Valone TJ, Templeton JJ, 2002 Potential disadvantages of using socially acquired information. *Philosophical Transactions of the Royal Society of London. Series B: Biological Sciences* **357**, 1559–1566
6. Rogers AR, 1988 Does biology constrain culture? *American Anthropologist* **90**, 819–831
7. Kendal RL, Boogert NJ, Rendell L, Laland KN, Webster M, Jones PL, 2018 Social learning strategies: Bridge-building between fields. *Trends in cognitive sciences* **22**, 651–665
8. Laland KN, 2004 Social learning strategies. *Animal Learning & Behavior* **32**, 4–14

9. Aoki K, Feldman MW, 2014 Evolution of learning strategies in temporally and spatially variable environments: a review of theory. *Theoretical population biology* **91**, 3–19
10. Giraldeau LA, Caraco T, 2000 *Social foraging theory*. Princeton University Press
11. Mesoudi A, O'Brien MJ, 2008 The cultural transmission of great basin projectile-point technology i: an experimental simulation. *American Antiquity* **73**, 3–28
12. Mesoudi A, 2008 An experimental simulation of the "copy-successful-individuals" cultural learning strategy: Adaptive landscapes, producer–scrounger dynamics, and informational access costs. *Evolution and Human Behavior* **29**, 350–363
13. Miu E, Gulley N, Laland KN, Rendell L, 2020 Flexible learning, rather than inveterate innovation or copying, drives cumulative knowledge gain. *Science advances* **6**, eaaz0286
14. McElreath R, Lubell M, Richerson PJ, Waring TM, Baum W, Edsten E, Efferson C, Paciotti B, 2005 Applying evolutionary models to the laboratory study of social learning. *Evolution and Human Behavior* **26**, 483–508
15. Deffner D, Kleinow V, McElreath R, 2020 Dynamic social learning in temporally and spatially variable environments. *Royal Society open science* **7**, 200734
16. Toyokawa W, Whalen A, Laland KN, 2019 Social learning strategies regulate the wisdom and madness of interactive crowds. *Nature Human Behaviour* **3**, 183–193
17. Toyokawa W, Gaissmaier W, 2022 Conformist social learning leads to self-organised prevention against adverse bias in risky decision making. *Elife* **11**, e75308
18. Witt A, Toyokawa W, Gaissmaier W, Lala K, Wu CM, 2023 Social learning with a grain of salt. *PsyArXiv*
19. Strandburg-Peshkin A, *et al.*, 2013 Visual sensory networks and effective information transfer in animal groups. *Current Biology* **23**, R709–R711
20. Wu CM, Deffner D, Kahl B, Meder B, Ho MH, Kurvers RH, 2023 Visual-spatial dynamics drive adaptive social learning in immersive environments. *bioRxiv*
21. Rahmani P, Peruani F, Romanczuk P, 2020 Flocking in complex environments—attention trade-offs in collective information processing. *PLoS computational biology* **16**, e1007697
22. Bastien R, Romanczuk P, 2020 A model of collective behavior based purely on vision. *Science advances* **6**, eaay0792
23. Vickery WL, Giraldeau LA, Templeton JJ, Kramer DL, Chapman CA, 1991 Producers, scroungers, and group foraging. *The american naturalist* **137**, 847–863
24. Barta Z, Flynn R, Giraldeau LA, 1997 Geometry for a selfish foraging group: a genetic algorithm approach. *Proceedings of the Royal Society of London. Series B: Biological Sciences* **264**, 1233–1238
25. Beauchamp G, 2008 A spatial model of producing and scrounging. *Animal Behaviour* **76**, 1935–1942
26. Kurvers RH, Hamblin S, Giraldeau LA, 2012 The effect of exploration on the use of producer-scrounger tactics. *PloS one* **7**, e49400
27. Deffner D, McElreath R, 2022 When does selection favor learning from the old? social learning in age-structured populations. *PloS one* **17**, e0267204
28. Leos-Barajas V, Michelot T, 2018 An introduction to animal movement modeling with hidden markov models using stan for bayesian inference. *arXiv preprint arXiv:1806.10639*
29. Auger-Méthé M, *et al.*, 2021 A guide to state–space modeling of ecological time series. *Ecological Monographs* **91**, e01470
30. Kass RE, Raftery AE, 1995 Bayes factors. *Journal of the american statistical association* **90**, 773–795
31. Kandler A, Powell A, 2018 Generative inference for cultural evolution. *Philosophical Transactions of the Royal Society B: Biological Sciences* **373**, 20170056
32. Rosati AG, 2017 Foraging cognition: reviving the ecological intelligence hypothesis. *Trends in cognitive sciences* **21**, 691–702
33. Kaplan H, Hill K, Lancaster J, Hurtado AM, 2000 A theory of human life history evolution: Diet, intelligence, and longevity. *Evolutionary Anthropology: Issues, News, and Reviews: Issues, News, and Reviews* **9**, 156–185
34. Henrich J, McElreath R, 2003 The evolution of cultural evolution. *Evolutionary Anthropology: Issues, News, and Reviews: Issues, News, and Reviews* **12**, 123–135
35. Henrich J, 2017 *The secret of our success: How culture is driving human evolution, domesticating our species, and making us smarter*. Princeton University Press
36. Schuppli C, Isler K, van Schaik CP, 2012 How to explain the unusually late age at skill competence among humans. *Journal of human evolution* **63**, 843–850
37. González-Forero M, Gardner A, 2018 Inference of ecological and social drivers of human brain-size evolution. *Nature* **557**, 554–557
38. Monk CT, Barbier M, Romanczuk P, Watson JR, Alós J, Nakayama S, Rubenstein DI, Levin SA, Arlinghaus R, 2018 How ecology shapes exploitation: a framework to predict the behavioural response of human and animal foragers along exploration–exploitation trade-offs. *Ecology letters* **21**, 779–793
39. Garg K, Kello C, Smaldino P, 2022 Individual exploration and selective social learning: Balancing exploration-exploitation trade-offs in collective foraging. *Journal of The Royal Society Interface* **19**
40. Hung AA, Plott CR, 2001 Information cascades: Replication and an extension to majority rule and conformity-rewarding institutions. *American Economic Review* **91**, 1508–1520
41. Bazazi S, von Zimmermann J, Bahrami B, Richardson D, 2019 Self-serving incentives impair collective decisions by increasing conformity. *PloS one* **14**, e0224725
42. Barbier M, Watson JR, 2016 The spatial dynamics of predators and the benefits and costs of sharing information. *PLoS computational biology* **12**, e1005147
43. Torney CJ, Berdahl A, Couzin ID, 2011 Signalling and the evolution of cooperative foraging in dynamic environments. *PLoS computational biology* **7**, e1002194
44. Berdahl A, Torney CJ, Ioannou CC, Faria JJ, Couzin ID, 2013 Emergent sensing of complex environments by mobile animal groups. *Science* **339**, 574–576
45. Hawkins RD, Berdahl AM, Pentland A, Tenenbaum JB, Goodman ND, Krafft P, *et al.*, 2022 Flexible social inference facilitates targeted social learning when rewards are not observable. *arXiv preprint arXiv:2212.00869*
46. Bidari S, El Hady A, Davidson JD, Kilpatrick ZP, 2022 Stochastic dynamics of social patch foraging decisions. *Physical review research* **4**, 033128
47. Brunswik E, 1955 Representative design and probabilistic theory in a functional psychology. *Psychological Review* **62**, 193–217.
48. Fawcett TW, Fallenstein B, Higginson AD, Houston AI, Mallpress DE, Trimmer PC, McNamara JM, 2014 The evolution of decision rules in complex environments. *Trends in Cognitive Sciences* **18**, 153–161.
49. Kihlstrom JF, 2021 Ecological validity and "ecological validity". *Perspectives on Psychological Science* **16**, 466–471
50. Adjerid I, Kelley K, 2018 Big data in psychology: A framework for research advancement. *American Psychologist* **73**, 899
51. Couzin ID, Heins C, 2022 Emerging technologies for behavioral research in changing environments. *Trends in Ecology & Evolution*
52. Garg K, Kello CT, 2021 Efficient lévy walks in virtual human foraging. *Scientific reports* **11**, 1–12
53. Spiers HJ, Coutrot A, Hornberger M, 2023 Explaining world-wide variation in navigation ability from millions of people: citizen science project sea hero quest. *Topics in cognitive science* **15**, 120–138
54. Moussaïd M, Perozo N, Garnier S, Helbing D, Theraulaz G, 2010 The walking behaviour of pedestrian social groups and its impact on crowd dynamics. *PloS one* **5**, e10047
55. Moussaïd M, Helbing D, Theraulaz G, 2011 How simple rules determine pedestrian behavior and crowd disasters. *Proceedings of the National Academy of Sciences* **108**, 6884–6888
56. Keshri S, Oh Mh, Zhang S, Iyengar G, 2019 Automatic event detection in basketball using hmm with energy based defensive assignment. *Journal of Quantitative Analysis in Sports* **15**, 141–153

57. Ali I, 2019. Tagging basketball events with hmm in stan. https://mc-stan.org/users/documentation/case-studies/bball-hmm.html. Accessed: 2023-05-03
58. Ötting M, Langrock R, Deutscher C, Leos-Barajas V, 2020 The hot hand in professional darts. *Journal of the Royal Statistical Society Series A: Statistics in Society* **183**, 565–580
59. Strandburg-Peshkin A, Farine DR, Couzin ID, Crofoot MC, 2015 Shared decision-making drives collective movement in wild baboons. *Science* **348**, 1358–1361
60. Strandburg-Peshkin A, Papageorgiou D, Crofoot MC, Farine DR, 2018 Inferring influence and leadership in moving animal groups. *Philosophical Transactions of the Royal Society B: Biological Sciences* **373**, 20170006
61. Pacheco-Cobos L, Winterhalder B, Cuatianquiz-Lima C, Rosetti MF, Hudson R, Ross CT, 2019 Nahua mushroom gatherers use area-restricted search strategies that conform to marginal value theorem predictions. *Proceedings of the National Academy of Sciences* **116**, 10339–10347
62. Wood BM, *et al.*, 2021 Gendered movement ecology and landscape use in hadza hunter-gatherers. *Nature Human Behaviour* **5**, 436–446
63. Ford JD, Tilleard SE, Berrang-Ford L, Araos M, Biesbroek R, Lesnikowski AC, MacDonald GK, Hsu A, Chen C, Bizikova L, 2016 Big data has big potential for applications to climate change adaptation. *Proceedings of the National Academy of Sciences* **113**, 10729–10732
64. Szocska M, *et al.*, 2021 Countrywide population movement monitoring using mobile devices generated (big) data during the covid-19 crisis. *Scientific Reports* **11**, 5943
65. Kays R, Crofoot MC, Jetz W, Wikelski M, 2015 Terrestrial animal tracking as an eye on life and planet. *Science* **348**, aaa2478
66. Kays R, *et al.*, 2022 The movebank system for studying global animal movement and demography. *Methods in Ecology and Evolution* **13**, 419–431
67. Nathan R, *et al.*, 2022 Big-data approaches lead to an increased understanding of the ecology of animal movement. *Science* **375**, eabg1780
68. Henrich J, Heine SJ, Norenzayan A, 2010 Most people are not weird. *Nature* **466**, 29–29
69. Deffner D, Rohrer JM, McElreath R, 2022 A causal framework for cross-cultural generalizability. *Advances in Methods and Practices in Psychological Science* **5**, 25152459221106366
70. Unity Technologies, 2021. Unity user manual. https://docs.unity3d.com/2020.3/Documentation/Manual/index.html. Accessed: 2023-05-03
71. Unity Technologies, 2021. Unity 2020.3.21. https://unity.com/releases/editor/whats-new/2020.3.21. Accessed: 2023-05-03
72. McElreath R, 2020 *Statistical rethinking: A Bayesian course with examples in R and Stan*. CRC press
73. McClintock BT, Langrock R, Gimenez O, Cam E, Borchers DL, Glennie R, Patterson TA, 2020 Uncovering ecological state dynamics with hidden markov models. *Ecology letters* **23**, 1878–1903
74. Bishop CM, Nasrabadi NM, 2006 *Pattern recognition and machine learning*, vol. 4. Springer
75. Bartumeus F, Campos D, Ryu WS, Lloret-Cabot R, Méndez V, Catalan J, 2016 Foraging success under uncertainty: search tradeoffs and optimal space use. *Ecology letters* **19**, 1299–1313
76. Zucchini W, MacDonald IL, Langrock R, 2017 *Hidden Markov models for time series: an introduction using R*. CRC press
77. Forney GD, 1973 The viterbi algorithm. *Proceedings of the IEEE* **61**, 268–278
78. Pewsey A, Neuhäuser M, Ruxton GD, 2013 *Circular statistics in R*. Oxford University Press
79. Carpenter B, Gelman A, Hoffman MD, Lee D, Goodrich B, Betancourt M, Brubaker M, Guo J, Li P, Riddell A, 2017 Stan: A probabilistic programming language. *Journal of statistical software* **76**
80. Gabry J, Češnovar R, 2020 cmdstanr: R interface to'cmdstan'. *See mc-stan. org/cmdstanr/reference/cmdstanr-package. html*
81. Lewandowski D, Kurowicka D, Joe H, 2009 Generating random correlation matrices based on vines and extended onion method. *Journal of multivariate analysis* **100**, 1989–2001
82. Vehtari A, Gelman A, Simpson D, Carpenter B, Bürkner PC, 2019 Rank-normalization, folding, and localization: An improved $\hat{R}$ for assessing convergence of mcmc. *arXiv preprint arXiv:1903.08008*
83. Gelman A, Rubin DB, *et al.*, 1992 Inference from iterative simulation using multiple sequences. *Statistical Science* **7**, 457–472
84. Gelman A, Carlin JB, Stern HS, Dunson DB, Vehtari A, Rubin DB, 2013 *Bayesian data analysis*. Chapman and Hall/CRC

Electronic Supplementary Material for

Collective incentives reduce over-exploitation of social information in unconstrained human groups

Dominik Deffner[1,2*], David Mezey[2,3], Benjamin Kahl[1], Alexander Schakowski[1], Pawel Romanczuk[2,3], Charley Wu[1,4,5] & Ralf Kurvers[1,2]

[1]Center for Adaptive Rationality, Max Planck Institute for Human Development, Berlin, Germany
[2]Science of Intelligence Excellence Cluster, Technical University Berlin, Berlin, Germany
[3]Institute for Theoretical Biology, Humboldt University Berlin, Berlin, Germany
[4]University of Tübingen, Tübingen, Germany
[5]Max Planck Institute for Biological Cybernetics, Tübingen, Germany
[*]deffner@mpib-berlin.mpg.de

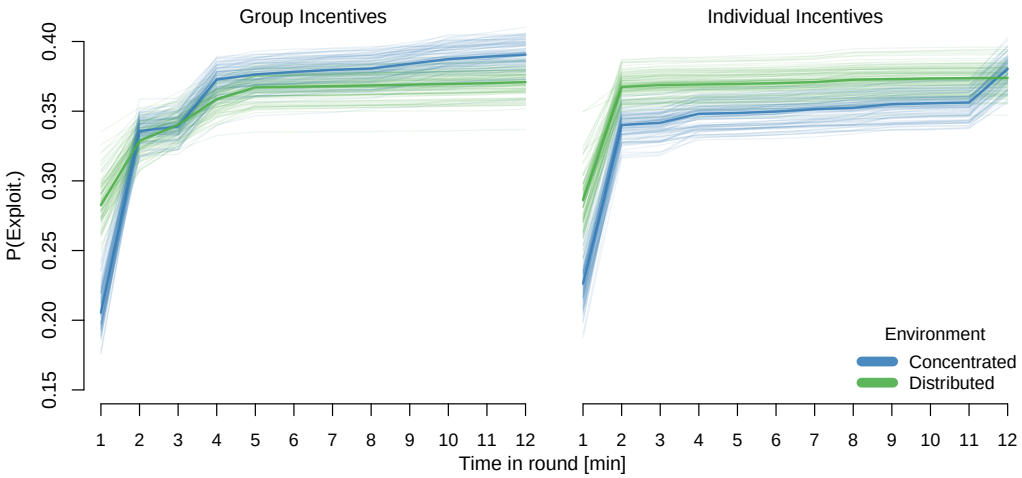

Figure 1. Exploitation probabilities over time 100 random draws from the posterior distribution (transparent lines) as well as posterior means (solid lines) for the probability that players are successful (i.e., exploiting a patch) over time per incentive condition and environment. Results come from multilevel logistic regression with time in round as an ordered categorical (monotonic) predictor.

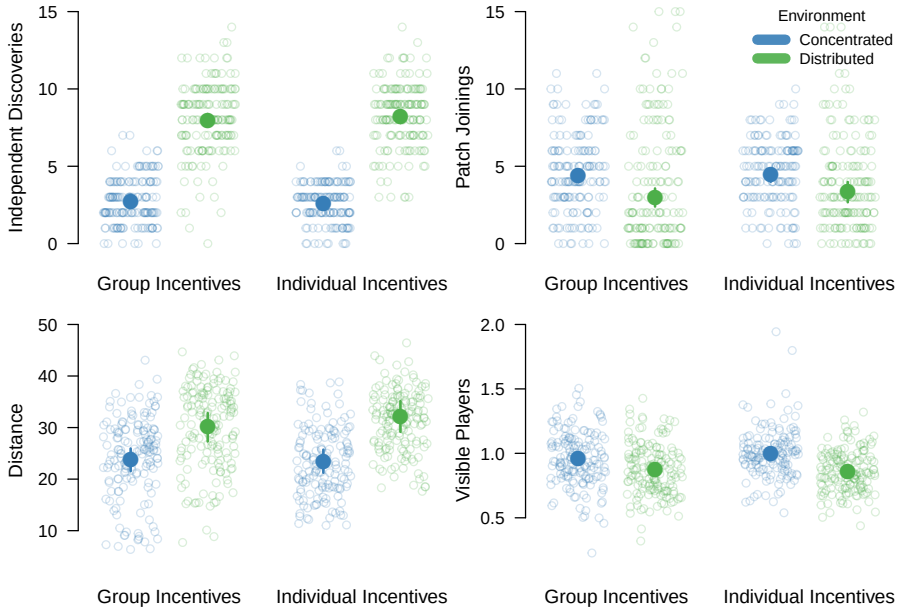

Figure 2. Additional behavioral results. Number of independent patch discoveries and patch joinings, as well as distance (average distance to the other three players for times when focal player was not exploiting) and visibility (average number of players in field of view when focal player was not exploiting). Each circle represents data from one round per participant, larger filled dots represent posterior estimates (as well as 90% HPDIs) from Bayesian multilevel models.

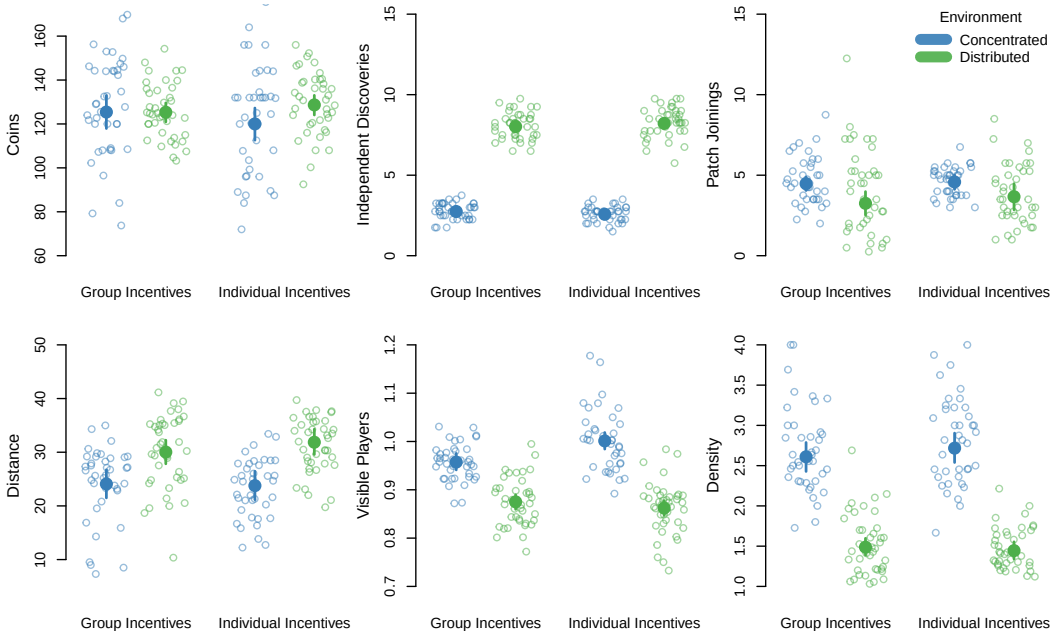

Figure 3. Behavioral results at the group level. Average number of coins collected, independent patch discoveries, patch joinings, distance (average distance to the other three players for times when focal player was not exploiting), visibility (average number of players in field of view when focal player was not exploiting), and density (average number of foragers exploiting at discovered patches) per environment and incentive condition. Each circle represents data from one round for each group of participants. Larger filled dots represent posterior estimates (as well as 90% HPDIs) from Bayesian multilevel models accounting for group-level variability.

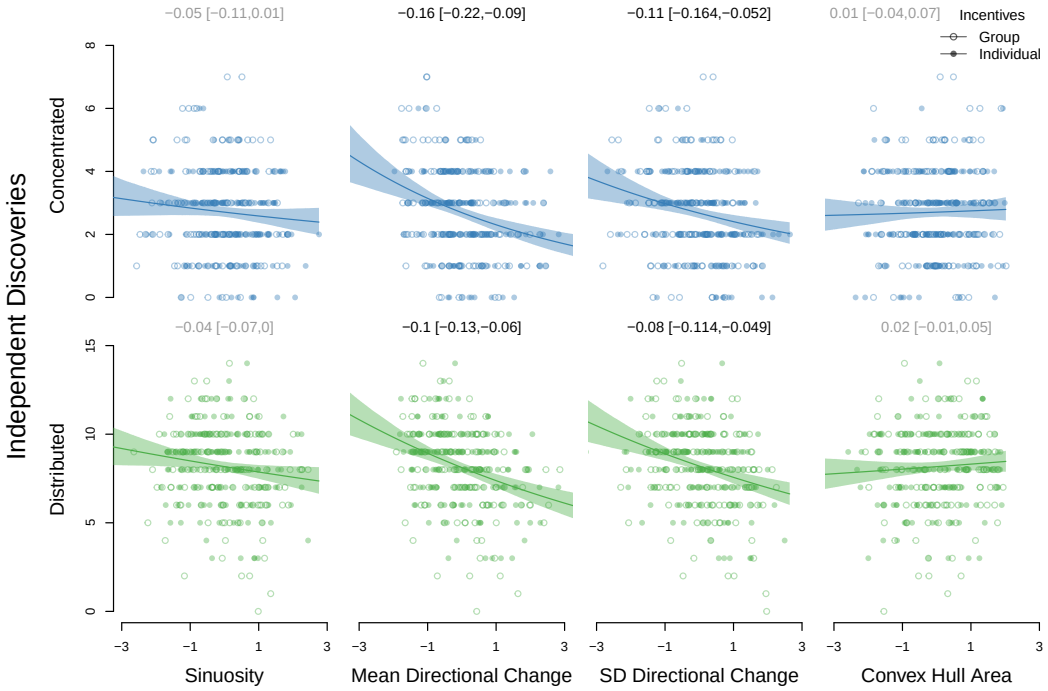

Figure 4. Movement metrics and independent discoveries. Number of patches independently discovered in each round by individuals in concentrated and distributed environments as a function of different metrics describing each movement trajectory (using the trajr r package by McLean and Skowron Volponi, 2018): (1) Sinuosity index (Benhamou, 2004), (2) the mean of directional changes (measure of nonlinearity), (3) the standard deviation of directional changes (measure of irregularity) (Kitamura and Imafuku, 2015) as well as (4) the convex hull area (area of smallest convex set containing all locations a participant visited). Open circles represent participants in the "Group Incentives" condition, filled circles represent participants in the "Individual Incentives" condition. Lines and uncertainty intervals show the effect of each variable (reported above, transparent text if 90% HPDI overlaps 0) from Bayesian Poisson regressions accounting for baseline differences between conditions. All predictors were z-standardized before the analysis.

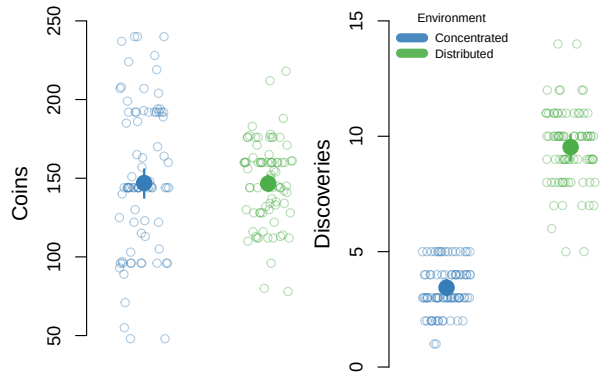

Figure 5. Behavioral results for individual foragers. Number of coins collected and independent patch discoveries for different environments. Each transparent circle represents data from one round for one participant. Larger filled dots represent posterior estimates (as well as 90% HPDIs) from Bayesian multilevel models.

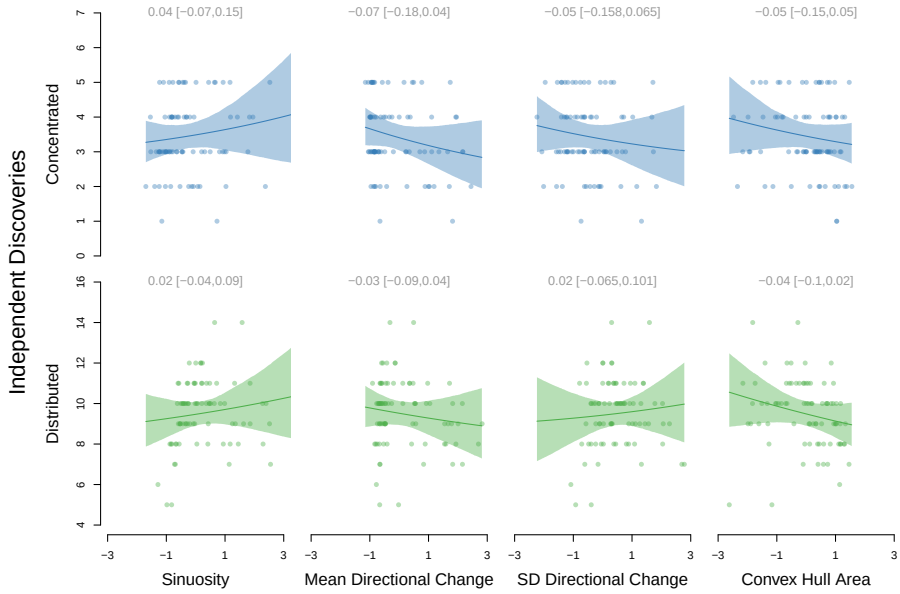

Figure 6. Movement metrics and independent discoveries for individual foragers. Number of patches discovered in each round by individuals in concentrated and distributed environments as a function of different metrics describing each movement trajectory (using the trajr r package by McLean and Skowron Volponi, 2018): (1) Sinuosity index (Benhamou, 2004), (2) the mean of directional changes (measure of nonlinearity), (3) the standard deviation of directional changes (measure of irregularity) (Kitamura and Imafuku, 2015) as well as (4) the convex hull area (area of smallest convex set containing all locations a participant visited). Lines and uncertainty intervals show the effect of each variable (reported above, transparent text if 90% HPDI overlaps 0) from Bayesian Poisson regressions. All predictors were z-standardized before the analysis.

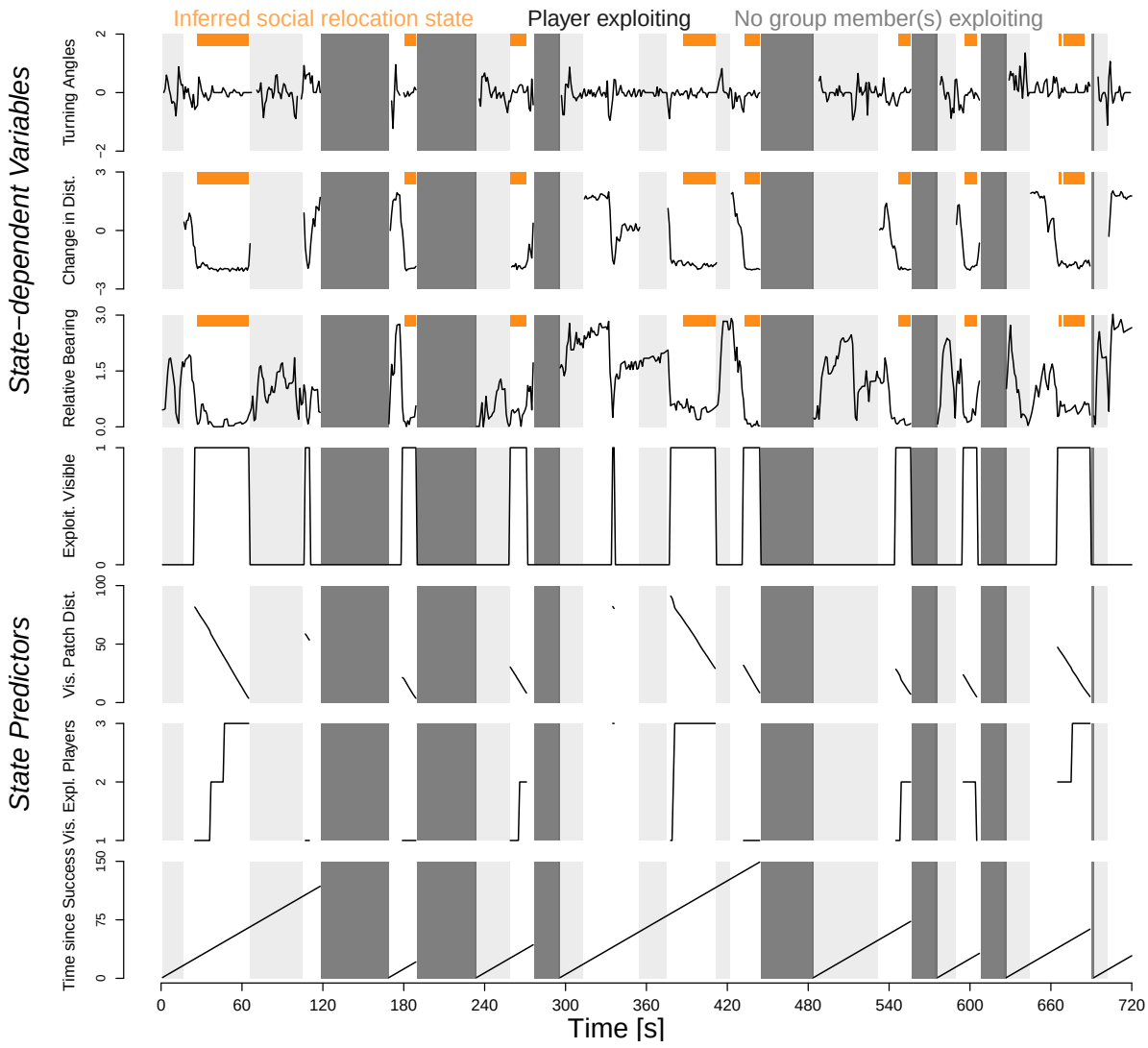

Figure 7. Exemplary time-series data for the Social Hidden Markov Decision Model. *State-dependent Variables* used to identify latent behavioral states include (1) turning angles (change in movement direction between successive time points; in radians), (2) (smallest) change in distance to exploiting player(s) across time points and (3) relative bearing (smallest angle between orientation vector of player and locations of other players). *State Predictors* used to model latent transition probabilities between behavioral states include (1) a binary visibility indicator V ("Is any exploiting player in field of view?"), (2) the distance to the closest visible exploited patch D, (3) the number of other players extracting at the closest visible patch N as well as (4) the time since the last success (coin extraction) T. Trajectories show one data point per second, the same temporal resolution as used in the computational model. Exploitation times when a player was collecting coins at a patch are marked by dark grey areas. Lighter grey areas represent periods when no other player was collecting coins. In both cases, we know the state of the focal player (exploitation and individual exploration, respectively), so we only explicitly model periods when players potentially could use social information. Orange bars represent time periods identified by the Viterbi algorithm as social relocation.

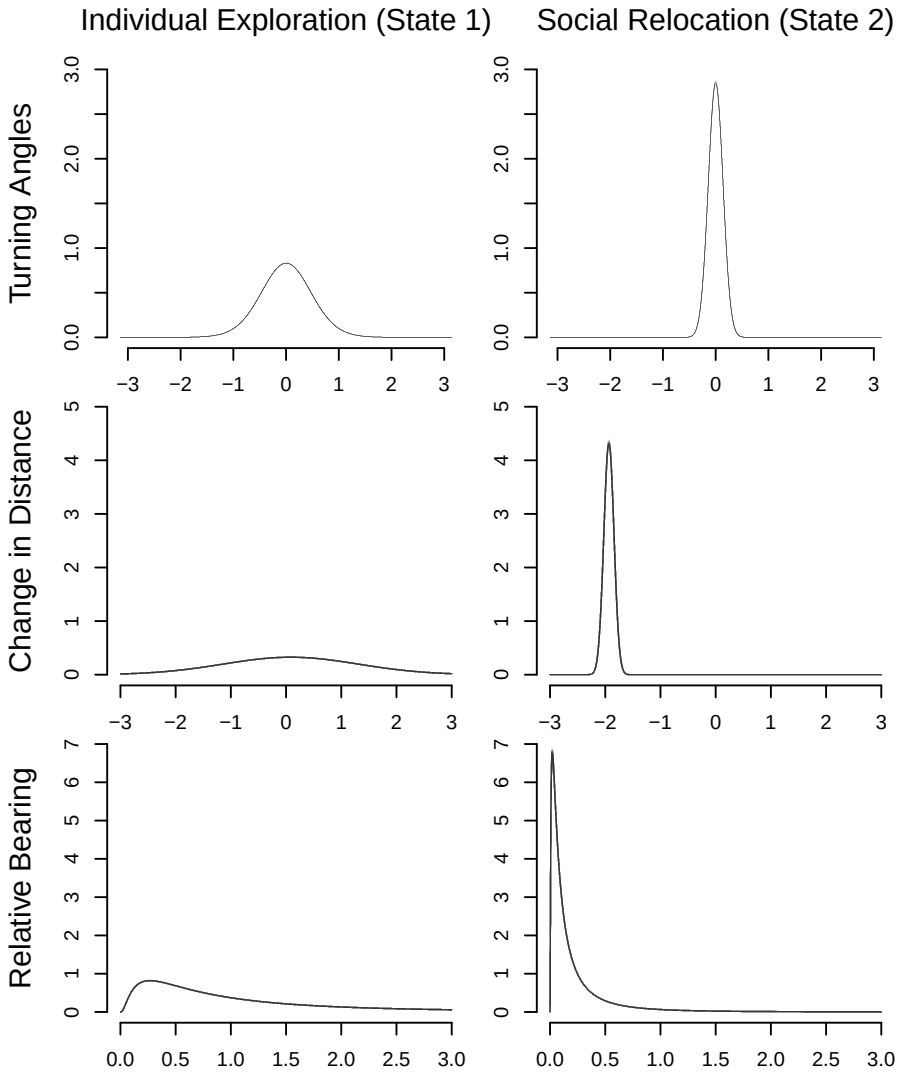

Figure 8. State-dependent distributions from the Social Hidden Markov Decision Model. Von Mises distributions for turning angles (top), Gaussian distributions for change in distance to exploiting players (middle) and lognormal distributions for relative bearing (bottom) based on 100 random draws from the posterior for state 1 ("Individual Exploration") and state 2 ("Social Relacation"). Lines look almost identical due to the very narrow posterior parameter estimates defining those distributions, which are derived from almost 150k observations. Note the greater variability in behavior during individual exploration results in substantially wider distributions for all three variables .

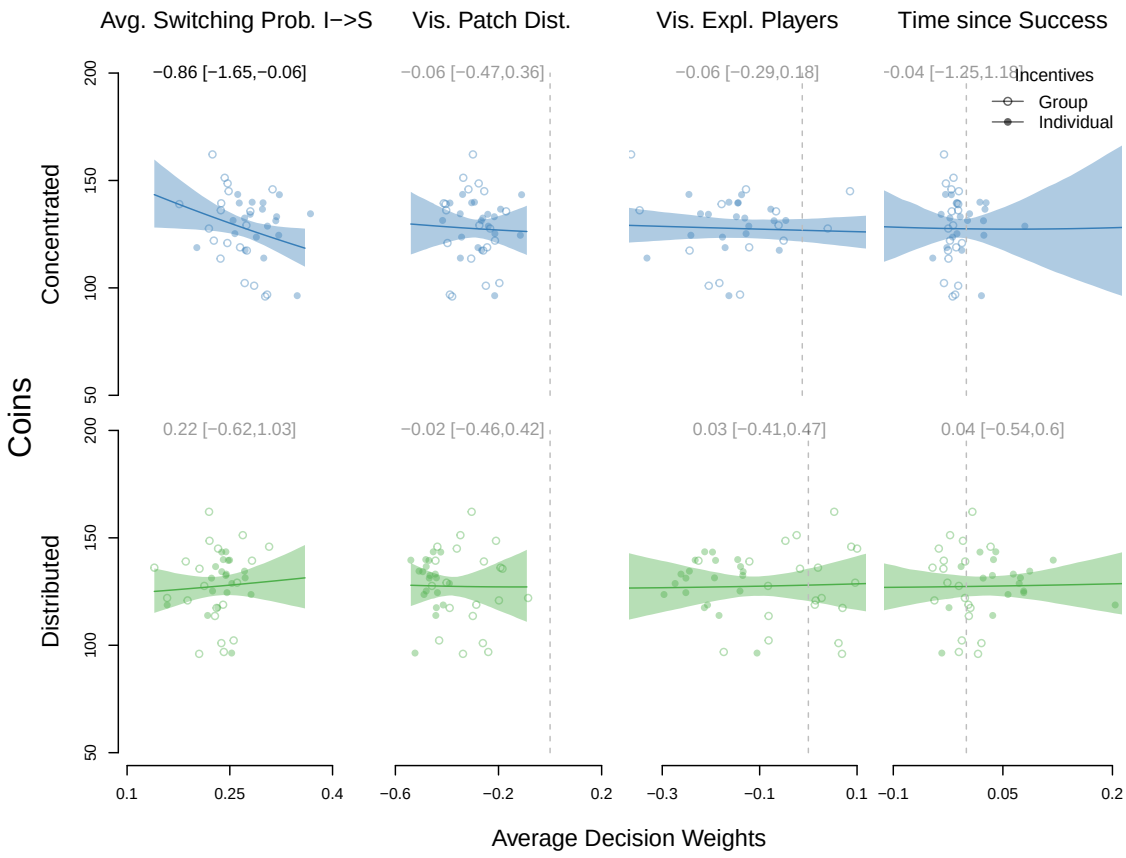

Figure 9. Influence of average decision weights on collective foraging success. Success (average number of coins collected by each group) in concentrated and distributed environments as a function of average individual-level weights derived from the Social Hidden Markov Decision Model. Open circles represent groups in the "Group Incentives" condition, filled circles represent groups in the "Individual Incentives" condition. Lines and uncertainty intervals show the effect of each decision weight (reported above, transparent text if 90% HPDI overlaps 0) from Bayesian log-normal regression models accounting for baseline success differences between conditions.

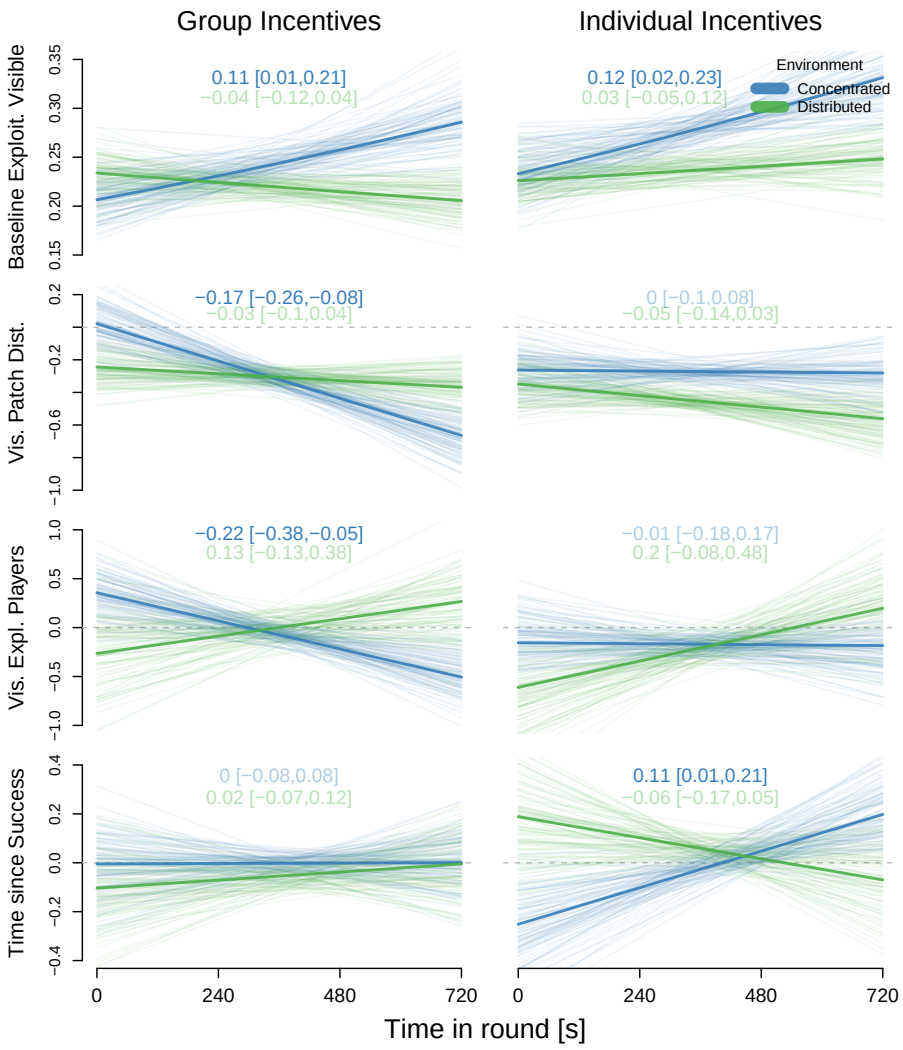

Figure 10. Computational modelling results: Temporal dynamics in state predictors using linear trends. 100 random draws from the posterior distribution (transparent lines) as well as posterior means (solid lines) for the influence of different state predictors over the course of experimental rounds. The top row shows baseline switching probabilities across all situations in which participants observe (a) successful player(s), the following rows show deviations from this expectation on the logit scale.

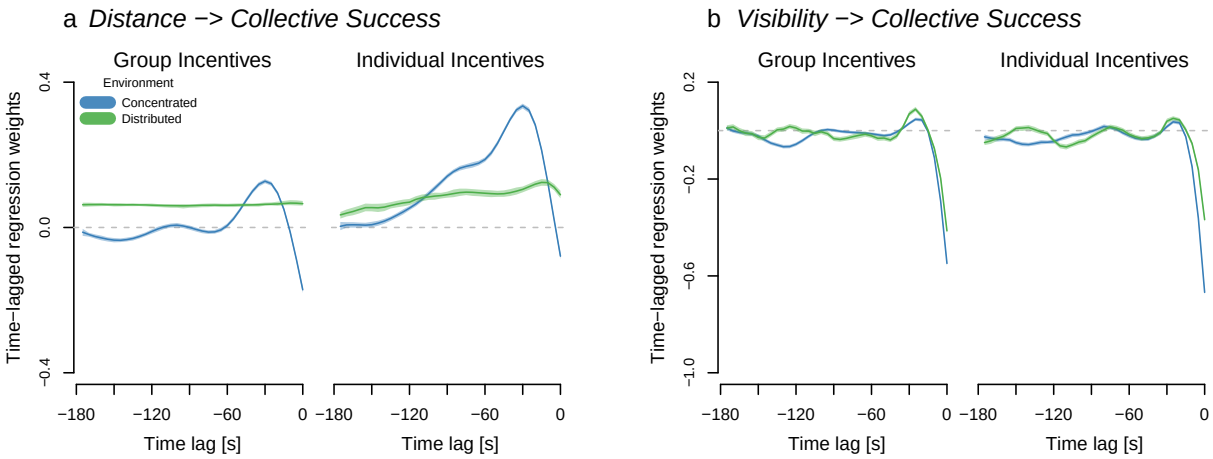

Figure 11. Collective visual-spatial dynamics for up to 3-minute time lags. Time-lagged Gaussian-process regression weights (including 90% HPDIs) predicting collective foraging success (number of players exploiting a patch) based on (a) distance (average pairwise distance among players) and (b) visibility (number of visual connections among group members, ranging from 0, where no one is looking at others, and 12, where everyone is looking at everyone else) across different time intervals per incentive condition and environment.

Table 1. Frequentist analysis: Coins collected per incentive condition and environment (Poisson likelihood, dummy-coded predictors)

	Estimate	SE	z	p-value
Intercept	4.01	0.01	394.21	$< 0.001^{***}$
Incentives	−0.04	0.01	−4.14	$< 0.001^{***}$
Environment	−0.01	0.01	−1.25	0.21
Incent. x Env.	0.07	0.02	4.95	$< 0.001^{***}$
Note:				*p<0.05; **p<0.01; ***p<0.001

Table 2. Expected number of coins collected (including 90% HPDIs) per environment (columns) depending on the environment in the previous round (rows). Results for group incentives are shown on the top, results for individual incentives are shown on the bottom.

Group Incentives

Previous	Concentrated	Distributed
First	125.0 [116.8, 133.5]	128.0 [122.6, 133.6]
Concentrated	124.7 [116.6, 133.2]	126.1 [121.6, 130.6]
Distributed	124.7 [116.9, 133.0]	118.6 [113.7, 123.6]

Individual Incentives

Previous	Concentrated	Distributed
First	121.8 [114.0, 130.0]	128.1 [122.8, 133.5]
Concentrated	109.8 [102.6, 117.2]	130.0 [125.4, 134.7]
Distributed	124.7 [116.9, 132.8]	125.5 [119.9, 130.2]

Table 3. Frequentist analysis: Discoveries per incentive condition and environment (Poisson likelihood, dummy-coded predictors)

	Estimate	SE	z	p-value
Intercept	1.06	0.07	15.24	$< 0.001^{***}$
Incentives	−0.06	0.07	−0.82	0.41
Environment	1.07	0.06	19.53	$< 0.001^{***}$
Incent. x Env.	0.08	0.08	1.04	0.30

Note: *p<0.05; **p<0.01; ***p<0.001

Table 4. Frequentist analysis: Joinings per incentive condition and environment (Poisson likelihood, dummy-coded predictors)

	Estimate	SE	z	p-value
Intercept	1.62	0.01	24.01	$< 0.001^{***}$
Incentives	−0.002	0.01	−0.03	0.97
Environment	−0.15	0.05	−2.69	0.007^{**}
Incent. x Env.	−0.04	0.07	−0.52	0.60

Note: *p<0.05; **p<0.01; ***p<0.001

Table 5. Frequentist analysis: Distance to others per incentive condition and environment (lognormal likelihood, dummy-coded predictors)

	Estimate	SE	z	p-value
Intercept	3.14	0.04	71.02	$< 0.001^{***}$
Incentives	−0.01	0.03	−0.37	0.71
Environment	0.24	0.03	6.96	$< 0.001^{***}$
Incent. x Env.	0.08	0.05	1.64	0.015^{*}
Note:				*p<0.05; **p<0.01; ***p<0.001

Table 6. Frequentist analysis: Visibility of others per incentive condition and environment (Gaussian likelihood, dummy-coded predictors)

	Estimate	SE	z	p-value
Intercept	0.96	0.03	34.64	$< 0.001^{***}$
Incentives	0.05	0.02	2.07	0.04^{*}
Environment	−0.08	0.02	−3.85	$< 0.001^{***}$
Incent. x Env.	−0.06	0.03	−1.90	0.058
Note:				*p<0.05; **p<0.01; ***p<0.001

Table 7. Frequentist analysis: Scrounging rate per incentive condition and environment (binomial likelihood, dummy-coded predictors)

	Estimate	SE	z	p-value
Intercept	0.49	0.09	4.99	$< 0.001^{***}$
Incentives	0.16	0.09	1.68	0.09
Environment	−1.59	0.07	−21.27	$< 0.001^{***}$
Incent. x Env.	−0.27	0.11	−2.51	0.012^{*}
Note:				*p<0.05; **p<0.01; ***p<0.001

References

Benhamou, S. (2004). How to reliably estimate the tortuosity of an animal's path:: straightness, sinuosity, or fractal dimension? *Journal of theoretical biology*, 229(2):209–220.

Kitamura, T. and Imafuku, M. (2015). Behavioural mimicry in flight path of batesian intraspecific polymorphic butterfly papilio polytes. *Proceedings of the Royal Society B: Biological Sciences*, 282(1809):20150483.

McLean, D. J. and Skowron Volponi, M. A. (2018). trajr: An r package for characterisation of animal trajectories. *Ethology*, 124(6):440–448.